





Lars Geurink^{1,2} 
 Ewoud van Tricht¹ 
 Debbie van der Burg¹ 
 Gerard Scheppink¹
 Bojana Pajic¹
 Justin Dudink¹
 Cari Sanger-van de
 Griend^{1,2,3} 

¹Janssen Vaccines and
Prevention B.V., CN Leiden, The
Netherlands

²Department of Medicinal
Chemistry, Faculty of Pharmacy,
Biomedical Centre, Uppsala
University, Uppsala, Sweden

³Kantisto B.V., Baarn, The
Netherlands

Received August 27, 2021

Revised October 14, 2021

Accepted October 25, 2021

Research Article

Sixteen capillary electrophoresis applications for viral vaccine analysis

A broad range of CE applications from our organization is reviewed to give a flavor of the use of CE within the field of vaccine analyses. Applicability of CE for viral vaccine characterization, and release and stability testing of seasonal influenza virosomal vaccines, universal subunit influenza vaccines, Sabin inactivated polio vaccines (sIPV), and adenovirus vector vaccines were demonstrated. Diverse CZE, CE-SDS, CGE, and cIEF methods were developed, validated, and applied for virus, protein, posttranslational modifications, DNA, and excipient concentration determinations, as well as for the integrity and composition verifications, and identity testing (e.g., CZE for intact virus particles, CE-SDS application for hemagglutinin quantification and influenza strain identification, chloride or bromide determination in process samples). Results were supported by other methods such as RP-HPLC, dynamic light scattering (DLS), and zeta potential measurements. Overall, 16 CE methods are presented that were developed and applied, comprising six adenovirus methods, five viral protein methods, and methods for antibodies determination of glycans, host cell-DNA, excipient chloride, and process impurity bromide. These methods were applied to support in-process control, release, stability, process- and product characterization and development, and critical reagent testing. Thirteen methods were validated. Intact virus particles were analyzed at concentrations as low as 0.8 pmol/L. Overall, CE took viral vaccine testing beyond what was previously possible, improved process and product understanding, and, in total, safety, efficacy, and quality.

Keywords:

Analytical quality by design / Application / CE / Validation / Virus vaccine

DOI 10.1002/elps.202100269



Additional supporting information may be found online in the Supporting Information section at the end of the article.

Correspondence: Lars Geurink, MSc., Janssen Vaccines and Prevention B.V., Archimedesweg 4–6, 2333 CN Leiden, The Netherlands.

Email: lgeurin1@its.jnj.com

Abbreviations: Ad26, adenovirus type 26; AEX, anion exchange; AQbD, analytical quality by design; AUC, analytical ultra-centrifugation; BFS, bare fused silica; CH, clarified harvest; CMA, critical material attribute; CMP, critical method parameter; CPP, critical process parameter; CS, control strategy; DB, domiphen bromide; DLS, dynamic light scattering; DP, drug product; DS, drug substance; ELS, electrophoretic light scattering; FB, formulation buffer; HA, hemagglutinin; HIV, human immunodeficiency virus; (i)cIEF, (imaging) capillary isoelectric focusing; IPC, in-process control testing; LH, lysed harvest; NIBSC, National Institute for Biological Standards and Control; PAR, proven acceptable range; PNGase F, N-glycosidase F; PTM, posttranslational modification; qPCR, quantitative polymerase chain reaction; RP-HPLC, reversed-phase high-performance liquid chromatography; RSV, respiratory syncytial virus; SDS, sodium dodecyl sulfate; SE, sedimentation equilibrium; sIPV, Sabin inactivated polio vaccine;

1 Introduction

Viral vaccines are key in the prevention of infectious diseases caused by viruses such as nCoV-2, Ebola virus, Respiratory syncytial virus (RSV), human immunodeficiency virus (HIV), influenza virus, Polio virus, and so on [1,2]. Vaccines must be proven safe, efficacious, and of constant quality, and must be authorized by health authorities before the vaccine can be administered [3]. Analytical methods are needed to prove safety, efficacy, and quality, by determining the product identity, product and process-related impurities, product content, and product potency [4]. First, vaccine products are characterized to determine the critical quality attributes (CQAs) of the vaccine that are linked to safety, efficacy, and quality. Second, the critical process parameters (CPPs) and the critical material attributes (CMAs) are determined, and proven acceptable

SRID, single radial immunodiffusion; SV, sedimentation velocity; UF/DF, ultra- and diafiltration; UV, ultraviolet

Color online: See article online to view Figs. 1–15 in color.

ranges (PARs) and design space are set [2,5–8]. Subsequently, a control strategy (CS) is defined. Analytical testing is vital to support this process for determining and linking CQAs, CPPs, CMAs, and PARs, and defining a CS.

Due to the nature of CE, that is, efficient, sensitive, and fast separation in small volumes, the technique is intrinsically suitable for analytical analysis for many different CQAs, e.g., virus content and integrity [9–32], viral protein content, composition, integrity, and identity [33–44], protein [45], chloride [46], bromide [47,48] excipients, etc. However, only a few publications are in the context of pharmaceutical analysis of viral vaccines.

The objective of this paper is to demonstrate the applicability of CE for viral vaccine analysis by presenting studies done within Janssen Vaccines. Application of CE was studied for viral vaccine characterization, and release and stability testing of seasonal influenza virosomal vaccines, universal subunit influenza vaccines, Sabin inactivated polio vaccines (sIPV), and adenovirus vector vaccines.

2 Materials and methods

If not indicated otherwise, samples were produced at Janssen Vaccines and Prevention (Leiden, the Netherlands). Antibody 1 (Ab1) and antibody 2 (Ab2) were from ImmunoPrecise antibodies Ltd. (Victoria, Canada). NIBSC B/Brisbane/60/2008 was from NIBSC (Hertfordshire, UK). Ad5.ATCC was from American Type Culture Collection (Manassas, USA).

All CE experiments were performed on an Agilent 7100 capillary *Electrophoresis* system (Waldbronn, Germany) with either ChemStation (Agilent) or Waters Empower 3 (Milford, USA) software, if not indicated otherwise.

2.1 CE-SDS analysis

A 50 μm ID bare-fused silica (BFS) capillary, total length of 33.0 cm and detection window at 24.5 cm from Agilent was used. The capillary was conditioned with 0.1 M NaOH at 4 bar for 10 min and 0.1 M HCl at 4 bar for 3 min, Milli-Q water at 4 bar for 2 min, and filled with gel buffer at 4 bar for 10 min from the IgG purity and heterogeneity assay kit from Sciex (Nieuwerkerk aan den IJssel, The Netherlands) [49]. All samples were injected at 100 mbar for 100 s. Separations were performed with a pressure of 2 bar on both capillary ends and an applied voltage of -20 kV. Signals were recorded at 214 nm.

2.1.1 CE-SDS for critical reagent antibody purity

Samples were treated according to the purity and heterogeneity assay kit [49]. Separation was achieved with an applied voltage of -16.5 kV, and a cassette temperature of 25°C .

2.1.2 CE-SDS for seasonal influenza protein

Samples were reduced and denatured with 0.5% (v/v) sodium dodecyl sulfate (SDS, Invitrogen Bleiswijk, The Netherlands) and 62.5 mM 2-mercapthoethanol (2-ME, Sigma Aldrich Zwijndrecht, The Netherlands), set to 100°C , for 10 min. Deglycosylation was performed by adding 4 μL of phosphate buffer pH 7.4, 4 μL of N-glycosidase F (PNGase F, Roche Woerden, The Netherlands), and 4 μL of Triton X-100 (Sigma Aldrich) to 20 μL of the reduced sample, and incubation at 37°C for 1 h. Before analysis, 2 μL of 10% (w/v) SDS was added to the deglycosylated sample. The samples were injected on either the short end, 8.5 cm effective length, or long end, 24.5 cm effective length (100 mbar for 100 s). Separation was achieved with a cassette temperature of 32.5°C , and 85% v/v gel buffer (kit gel buffer diluted with Milli-Q water). See van Tricht et al. for more details [33].

2.1.3 CE-SDS for universal influenza protein

Samples were reduced and denatured with 0.45% w/v SDS and 4.5% v/v 2-ME and incubated at 70°C for 10 min and subsequently deglycosylated using 0.66% v/v Triton X-100, 6.6% of a mixture of deglycosylation enzymes consisting of PNGase F, O-glycosidase (New England Biolabs Evry, France), and neuraminidase from *Arthrobacter ureafaciens* (Sigma-Aldrich), and incubated at 37°C for 1 h. Before analysis, 0.32% w/v SDS and 1.6% v/v 10 kDa internal standard (Sciex) were added. Samples were injected (100 mbar for 100 s) at the short-end of the capillary, 8.5 cm effective length. The capillary temperature was kept at 20°C . See Geurink, et al. for more details [34].

2.1.4 CE-SDS for Sabin inactivated polio protein

Samples were reduced and denatured with 2% w/v SDS and 7% v/v 2-ME and incubated at 100°C for 20 min. Samples were injected (100 mbar for 100 s) at the long end of the capillary, 24.5 cm effective length. The separation conditions were 20°C capillary temperature, and 80% v/v gel buffer. See Geurink et al. for more details [34].

2.2 icIEF for universal influenza protein

Imaging capillary isoelectric focusing (icIEF) analyses were performed on a Maurice C. instrument (ProteinSimple San Jose, USA). Sialic acids were removed by the addition of 1.3% v/v sialidase from *Arthrobacter ureafaciens* (Sigma-Aldrich) to the sample and incubation for 2 h at 37°C . Subsequently, the samples were buffer exchanged and concentrated on a 10 kDa Amicon spin filter (MilliPore Merck Amsterdam-Zuidoost, the Netherlands). The icIEF separation master mix for one sample was composed of 2 μL Pharmalyte pI 3–10 (GE Healthcare Chicago, USA), 6 μL Servalyt pI 4–9 (Biophoret-

ics Spars, USA), 70 μL 1% methylcellulose (ProteinSimple), 34 μL Milli-Q water, 2 μL Maurice C. pI marker 3.38 (ProteinSimple), 2 μL Maurice C. pI marker 7.05 (ProteinSimple), 5 μL 1.5 M urea solution (Sigma–Aldrich), and 11 μL Anodic spacer 200 mM iminodiacetic acid (Sigma–Aldrich). Equilibration and rinsing were performed using default Maurice C conditions. Twenty-five microliters of sample was mixed on-board with 100 μL of master mix and run at 1 min 1500 V and 6 min 3000 V. Native protein fluorescent signals were used for peak integration and apparent pI determination.

2.3 CZE for adenovirus analysis

A PVA coated capillary with extended light path, 50 μm ID, 33.0 cm total length, and 8.5 cm effective length (Agilent) was rinsed with 10 mM ortho-phosphoric acid (Merck Millipore) and filled with a BGE (pH 7.7) composed of a 125 mM Tris(hydroxymethyl)aminomethane (Merck Millipore), and 338 mM tricine (Sigma Aldrich), and 0.2% polysorbate-20 (Merck Millipore), both at 2.5 bar for 1 min. Samples were injected at 50 mbar for 5 s at the short end of the capillary (8.5 cm effective length) and separated with an applied voltage of -25 kV (12 s ramping) at 15°C cassette temperature. UV-absorbance at 214 nm was recorded. See for more details van Tricht et al. [20]. The adenovirus type 26 (Ad26) concentration was determined based on the corrected peaks area and a one-point calibration from a well-characterized in-house Ad26 reference material.

2.4 HC DNA analysis

DNA was purified from the samples using the DNA extractor WAKO kit (Fujifilm Neuss, Germany) [50]. To 500 μL of sample, 20 μL of sodium N-lauroyl sarcosinate solution, and 500 μL sodium iodide with glycogen were added and incubated for 15 min at 40°C. The sample was centrifugated at 10.000 g for 15 min. The supernatant was removed and the pellet was reconstituted in formulation buffer (FB).

2.4.1 Capillary gas electrophoresis

Analysis was performed according to the Sciex dsDNA 1000 kit [51]. A Sciex 8000 plus system was used with a Sciex DNA Capillary (100 μm ID, 40.2 cm total length, 30 cm effective length). The capillary was conditioned with dsDNA gel at 20 psi for 10 min, water dip for 0 min, and applied voltage at -5.0 kV for 10 min (with a 5 min ramp). Before each sample injection, the capillary was conditioned with the Sciex DSFNDA 1000 Gel Buffer with LIFluor™ Enhance dye at 20 psi for 10 min. The Thermo Fisher Scientific 200 bp (Breda, The Netherlands) was added as an internal standard to the sample and the sample was injected at -8 kV for 20 s. Separation was performed with an applied voltage of -7.8 kV, at 20°C, for

30 min. The fluorescent signal was recorded with excitation wavelength of 488 nm and emission wavelength of 520 nm.

2.4.2 Slab-gel electrophoresis

Slab-gel electrophoresis was performed according to the Bio-Rad Chemidoc user guide [52]. Lonza (Geleen, The Netherlands) 6x loading buffer was added to the samples 1:5 (v:v) and loaded on a Lonza Flash Gel cassette 2.2% agarose loading gel. Separation was performed on a Bio-Rad (Lunteren, The Netherlands) ChemiDac gel Electrophoresis instrument at 250 V for 6 min. Pictures were made with the Bio-Rad camera and processed with the Bio-Rad Image Lab software.

2.5 DLS and ELS

The determinations of the size and zeta potential of adenovirus particles were performed with a Malvern Panalytical Ltd. (Malvern, UK) Zetasizer Nano ZS. Measurements were carried out at 25°C with a disposable Folded Capillary cell (DTS 1070, Malvern Panalytical Ltd.) containing 800 μL sample. The size determination was measured by dynamic light scattering (DLS) with a 632.8 nm laser at a measuring angle of 173°. The laser power was set on automatic attenuation. For each size determination, a total of three measurements were performed, the measurement duration was set on automatic. The zeta potential was measured by electrophoretic light scattering (ELS). The zeta potential was determined by measuring the electrophoretic mobility with electrophoretic light scattering and converting this value into the zeta potential using the Smoluchowski equation. A total of three measurements consisting of 20 runs each were performed. The laser attenuation and the voltage selection were set on automatic. Data acquisition and processing were done by the Zetasizer software.

2.6 Domiphen concentration with RP-HPLC-CAD

Reversed-phase high-performance liquid chromatography (RP-HPLC) analyses were carried out on a Waters Alliance 2695 HPLC with a Waters XBridge™ Shield RP18 column (4.6×100 mm, 3.5 μm), with mobile phases A: 10 mM ammonium acetate (Sigma Aldrich), pH 3, and B: acetonitrile (Sigma Aldrich). One hundred microliters sample was injected and elution was carried out at a flow rate of 1.0 mL/min starting with 5% B for 2.2 min, followed by a linear gradient of 1.8 min to 95% B and 95% B for 2 min. Column re-equilibration comprised a linear gradient of 95% to 5% B in 1 min followed by 5% B for 2 min. The column temperature was 60°C. Analytes were monitored with a UV detector at 262 nm. Data acquisition and processing were done by Empower 3 software. The concentration was determined based on the peak area and a calibration curve prepared with weighted in domiphen standards.

2.7 CZE for bromide analysis

An Agilent BFS capillary, with an extended light path, 50 μm ID, and a 48.5 cm total length (40 cm effective length), was used. The capillary was flushed at 1 bar with 0.1 M sodium hydroxide for 10 min and Milli-Q water for 2 min and equilibrated until 20°C before analysis. Before each injection, the capillary was flushed at 1 bar with Milli-Q water for 1 min, 60% v:v acetonitrile in Milli-Q water for 2 min, and the BGE for 3 min (100 mM methane-sulfonic acid (Sigma–Aldrich), 74 mM triethanolamine (Sigma–Aldrich), 60% v:v acetonitrile (Sigma–Aldrich)). Samples were diluted five times in MS-water (Biosolve Valkenswaard, The Netherlands) and injected at 100 mbar for 5 s. Separation was performed with an applied voltage of -15 kV at 20°C (ramped to -15 kV in 30 s). UV-absorbance at 200 nm was recorded. The bromide concentration was determined based on the corrected peak area and a three-point calibration curve of potassium bromide (Sigma Aldrich) in MS-grade water standards.

2.8 CZE for Chloride analysis

Analysis was performed according to the CZE method for adenovirus analysis (see Section 3.2) with an analysis time of 1 min. The chloride concentration was determined based on the corrected negative peak area and a three-level calibration curve prepared from sodium chloride (Merck) in Milli-Q standards.

2.9 RP-HPLC for Ad26 protein analysis

A Waters Acquity H-class UPLC system with PDA detector, quaternary solvent manager, and autosampler with a Waters Acquity UPLC protein BEH C4 column, 2.1 mm diameter, 150 mm length, 300 Å pore size, and 1.7 μm particle diameter were used. New columns were conditioned with 3 injections of cytochrome c (Sigma–Aldrich). Samples were injected and proteins separated through a gradient from 20% - 60% v:v acetonitrile in 17 min, with a continuous TFA (Biosolve) concentration of 0.175% w/v. UV-absorbance at 280 nm was recorded and peaks were integrated to determine retention times and %peak areas. Peaks were identified with fraction collection and peptide mapping procedure with trypsin digestion and LC-MS^E analysis. See for more details van Tricht et al. [53].

3 Results and discussion

In general, we have found CE suitable for a wide range of applications within vaccine analysis. Here, we describe sixteen CE methods that were developed, of which thirteen were validated, see Table 1 for the list of applications and validation results, and see supporting information for

validation result tables and the statistical procedures. The applications include the analysis of critical reagent antibody purity, seasonal virosomal influenza vaccine, universal subunit influenza vaccine, Sabin inactivated polio vaccine (sIPV), and adenovirus vector vaccines. For the adenovirus vector vaccine applications, applications during different steps of the process, i.e., seed production, cell lysis, clarification, anion exchange (AEX)-filtration, ultra- and diafiltration (UF/DF), and drug substance (DS) and drug product (DP), are described.

3.1 Critical reagents antibody purity

For many vaccine products, product identity and potency are determined as part of product release testing. Often, antibodies are being used in assays for the determination of potency and identity. Antibodies are highly selective due to their structure and posttranslational modifications (PTMs). Antibodies are hard to produce at consistent quality and are prone to degradation [54], which consequently impacts the selectivity for the antigen. Therefore, antibodies are seen as critical reagents [55] and the quality of the antibody needs to be determined and controlled before use in a potency or identity test.

CE-SDS and cIEF are techniques that can be used to determine antibody molecular size and isoform patterns and were extensively used for antibody analysis previously (e.g., [56,57]). CE-SDS is a specific form of CGE where proteins are denatured with SDS and separation is based on size. CE-SDS can be used to determine the size variants of an antibody and is sensitive to for example fragmentation. cIEF can be used to determine charge variants and is sensitive to oxidation and loss of charged PTMs like sialic acids.

Although many publications discuss the use of CE-SDS and cIEF for therapeutic antibodies, we have used these techniques for the analysis of antibodies that are critical reagents for release testing technologies such as Western Blot (WB) identity testing and ELISA potency testing. As an example, the quality of HIV antibodies used for these tests was determined with CE-SDS. Multiple and broad light chain (LC) and heavy chain (HC) peaks were observed for Ab1 and Ab2, see Figure 1. This suggested heterogeneous Ab materials. This was not observed for Ab3. In parallel, antibody specificity was tested with WB and ELISA. Both Ab1 and Ab2 resulted in nonspecific bands with WB and background signals with ELISA in the presence of cell lysates and other HIV vaccine antigens. Ab3 resulted in one band at the expected location for WB and no significant background signal for ELISA in the presence of cell lysates and other HIV vaccine antigens. Therefore, the heterogeneous antibody materials could not be used for release testing, and Ab3 was selected for further WB and ELISA method development. The results of CE-SDS and cIEF analysis were used to improve antibody selection and control antibody quality as these kit-based applications proved to be quick and easy to apply, see Table 1 application 1.

Table 1. List of CE applications for viral vaccine analysis

Application #	Product	CE mode	Type of target	Target	Method status	Type of assay	Method application	Method performance characteristics
1	Critical method reagent	CE-SDS	Protein (antibody)	Primary antibody	Developed	Purity	Critical method reagent integrity	
2	Seasonal influenza	CE-SDS	Protein (viral)	Hemagglutinin subunit 1	Validated	Content	Product and process development and characterization	Repeatability 8%–10% RSD, accuracy 93%–109% compared to SRID, linearity $r^2 = 0.99$, range 7–76 $\mu\text{g/mL}$ HA [33]
3	Seasonal influenza	CE-SDS	Protein (viral)	Influenza Matrix protein, Nuclear protein, Hemagglutinin subunit 2	Developed	Content	Product and process development and characterization	Repeatability 1.9%–7.9% RSD, linearity $r^2 = 0.96$ –0.99, LOQ: 7 μg HA/mL [33]
4	Universal subunit influenza vaccine	CE-SDS	Protein (viral)	Hemagglutinin-stem based antigen [67–70]	Validated	Purity	Product and process development and characterization, stability indicating	Repeatability 0.8% RSD, Accuracy 99%–101%, Linearity $r^2 = 1.00$, range 0.50–3.13 mg/mL [34]
5	Universal subunit influenza vaccine	CE-SDS	PTM	Hemagglutinin-stem based antigen glycans [67–70]	Developed	Purity (quantitative)	Product and process development and characterization	
6	Universal subunit influenza vaccine	clEF	Protein (viral)	Hemagglutinin-stem based antigen [67–70]	Validated	Purity (quantitative)	Product and process development and characterization, stability indicating	Repeatability p/0.0%–0.7% RSD, repeatability % peak area 0.5%–0.7% RSD, LOQ < 0.1 mg mini-HA/mL, Supporting Information Table S1?
7	Sabin inactivated polio vaccine	CE-SDS	Protein (viral)	Polio virus protein 1–4	Validated	Identity	Product characterization	Repeatability area 8%–16% RSD, intermediate precision migration time 0.4%–0.8% RSD, linearity $r^2 = 0.98$, LOD 10 μg sIPV/mL [34]
8	Adenovirus vector vaccine	CZE	Virus	Adenovirus	Validated	Content	Release (Seed)	Repeatability 1.4%–4.2% RSD, intermediate precision 5.1%–9.3% RSD, accuracy 91%–103%, linearity 0.98–1.06 90% C.I. on the slope, range 2.5×10^{10} – 1.4×10^{11} VP/mL, Supporting Information Table 2
9	Adenovirus vector vaccine	CZE	Virus	Adenovirus	Validated	Content	In process control	Repeatability 0.7%–5.4% RSD, intermediate precision 1.8%–7.4% RSD, reproducibility 2.8%–5.4% RSD, accuracy 99%–110%, linearity 0.97–1.09 90% C.I. of the slope, range 6.7×10^{10} – 3.0×10^{12} VP/mL, Supporting Information Table 3

(Continued)

Table 1. (Continued)

Application #	Product	CE mode	Type of target	Target	Method status	Type of assay	Method application	Method performance characteristics
10	Adenovirus vector vaccine	CZE	Virus	Adenovirus	Validated	Content	Release and stability (DS/DP), stability indicating	Repeatability 0.9%–3.3% RSD intermediate precision 1.7%–5.1% RSD, accuracy 100%–104%, linearity 0.99–1.00 90% C.I. of the slope, range 2.5×10^{10} – 1.9×10^{11} VP/mL, Supporting Information Table 4
11	Adenovirus vector vaccine	CZE	Virus	Adenovirus	Validated	Content	Product and process development and characterization, stability indicating	Intermediate precision < 10% RSD Reproducibility < 6% RSD, accuracy 90%–110%, linearity 0.99–1.03 90% CI of the slope Range 2.0×10^{10} – 2.5×10^{12} VP/mL, [19]
12	Adenovirus vector vaccine	CZE	Virus	Adenovirus	Validated	Content	Process development (cell lysis)	Repeatability 0.7%–9.2% RSD, intermediate precision 0.8%–12% RSD, accuracy 94%–101%, linearity 0.99–1.01 90% CI of the slope, range 2.5×10^{10} – 1.4×10^{11} VP/mL, Supporting Information Table 5
13	Adenovirus vector vaccine	CGE	Nucleotides	Host cell DNA	Validated	Purity (quantitative)	Process development support	Repeatability 0.0%–2.4% RSD, Accuracy 98%–102% of mean value of ≤ 200 bp, Supporting Information Table 9
14	Adenovirus vector vaccine	CZE	Impurity	Br ⁻	Validated	Content	Process development support and validation	Repeatability 4.5%–10.5% RSD, intermediate precision 1.6%–21% RSD, accuracy 99%–107%, linearity 0.95–1.03 90% CI of the slope, range 5–100 μ M, LOQ 0.2 μ g/mL, Supporting Information Table 8
15	Product independent	CZE	Excipient	Cl ⁻	Validated	Content	Process development support and validation	Repeatability 1.8%–4.6% RSD, intermediate precision 2.2%–5.3% RSD, accuracy 90%–104%, linearity: 0.93–1.01 90% CI of the slope, range 38–113 mM, Supporting Information Table 7
16	Adenovirus vector vaccine	CZE	Virus	Adenovirus	Validated	Content	Low dose vaccine development support	Repeatability 2.3%–6.3% RSD, intermediate precision 2.3%–7.8% RSD, accuracy 95%–108%, linearity r^2 1.00, 1.00–1.06 90% CI of the slope, range 5×10^9 – 3.7×10^{11} VP/mL, Supporting Information Table 6

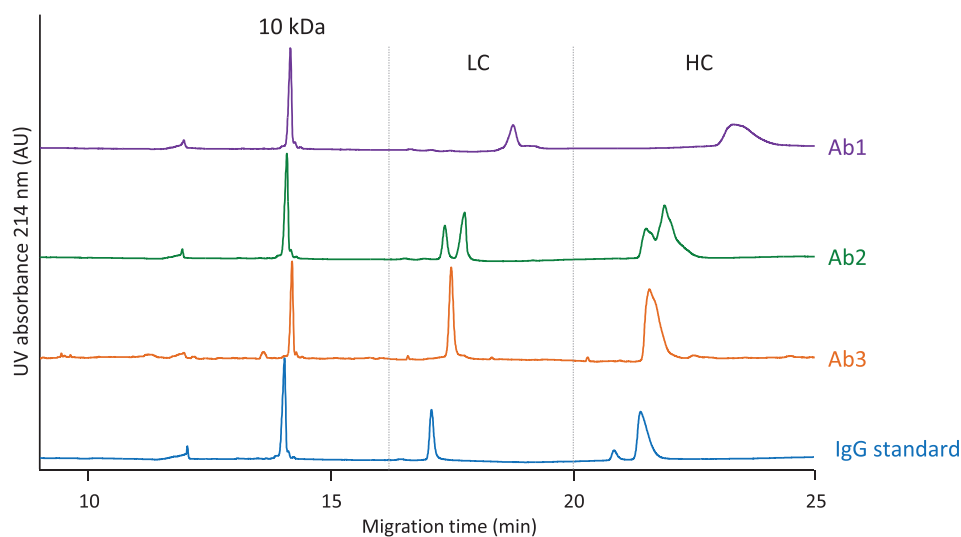


Figure 1. Critical antibody method reagent integrity testing of three HIV antibodies (Ab1, Ab2, and Ab3) with CE-SDS. The 10 kDa control standard is used as an internal standard and the light chains (LC) and heavy chains (HC) migration time ranges are depicted with dotted lines. For other conditions, see text.

3.2 Seasonal virosomal influenza vaccine

In addition to antibody analysis, the CE-SDS application developed for antibodies could be used for viral proteins as well [33,34,58–61]. For influenza vaccines, hemagglutinin (HA) is the most targeted influenza protein due to its immunogenic properties [62,63]. Due to the antigenic drift of HA, a new influenza vaccine with three different HA proteins needs to be developed each year. Usually, SDS-PAGE, single radial immunodiffusion (SRID) assays, and RP-HPLC methods were developed for identification and quantification. SDS-PAGE could not distinguish between different viral strains, could not quantify HA, and has low throughput. In addition, antibody selection for SRID is time consuming. RP-HPLC was not able to determine the HA concentration in complex matrices such as cell lysate and lacked precision and accuracy. For these reasons, a CE-SDS application was developed and validated (see Table 1 application 2) to quantify HA and identify the influenza strains. Potentially, the presence of other important proteins, such as neuraminidase (NA) [64,65], and matrix protein (M) [66], could be quantified as well [33], see Table 1 application 3. The method was further developed as short-end injection was tested to reduce analysis time and increase sample analysis throughput. The separation time decreased about threefold without significant loss of method performance, see Figure 2.

3.3 Universal subunit influenza vaccine “mini-HA”

3.3.1 Mini-HA size purity

A universal influenza vaccine is being developed to avoid yearly redevelopment or the risk of potential off-target vaccines. The universal influenza vaccine, “mini-HA,” is an HA-stem-based antigen called mini-HA and induces a broad-spectrum antibody response to cover many different

influenza HA variations [67–70]. For the development and the production of a group 1 mini-HA, a quantitative protein purity method was needed to determine peptide backbone integrity. With the four-step approach described previously [34] and based on the Sciex CE-SDS application, we were able to develop and validate a CE-SDS method for group 1 mini-HA purity determination ([34], Table 1 application 4).

3.3.2 Mini-HA PTM heterogeneity

The mini-HA protein is a homotrimer protein linked by disulfide bridges and has several *N*-linked and one *O*-linked glycosylation sites per monomer, with potentially multiple sialic acids attached per glycan. Glycans could have a significant effect on safety and efficacy due to their effect on the folding and shielding of functional epitopes [71,72].

Glycans are known to affect the CE-SDS separation [73,74] and CE-SDS was used for glycoprotein analysis previously [38]. Therefore, the optimized CE-SDS method to determine the mini-HA protein by its primary structure required an optimal sample preparation protocol to reduce and deglycosylate the protein. Reduced and nonreduced samples were tested with combinations of different glycosidases. Different combinations of glycosidases resulted in different peak patterns, see Figure 3.

Analysis of only denatured mini-HA (Figure 3B) caused a broad peak around 35 min which represented glycosylated trimeric mini-HA. The peak was only partly captured as the analysis run time was 35 min. Mini-HA reduction (Figure 3C) resulted in a broad hump composed of several peaks of glycosylated monomers at around 23 min. PNGase F treatment (Figure 3D) removed the *N*-glycans and resulted in 4 peaks in the time window of 25–30 min, and 2 peaks in the time window 15–20 min under non-reduced conditions. The 4 peaks around 25–30 min were likely trimeric mini-HA with 0, 1, 2, or 3 *O*-glycans attached. The 2 peaks around 15–20 min

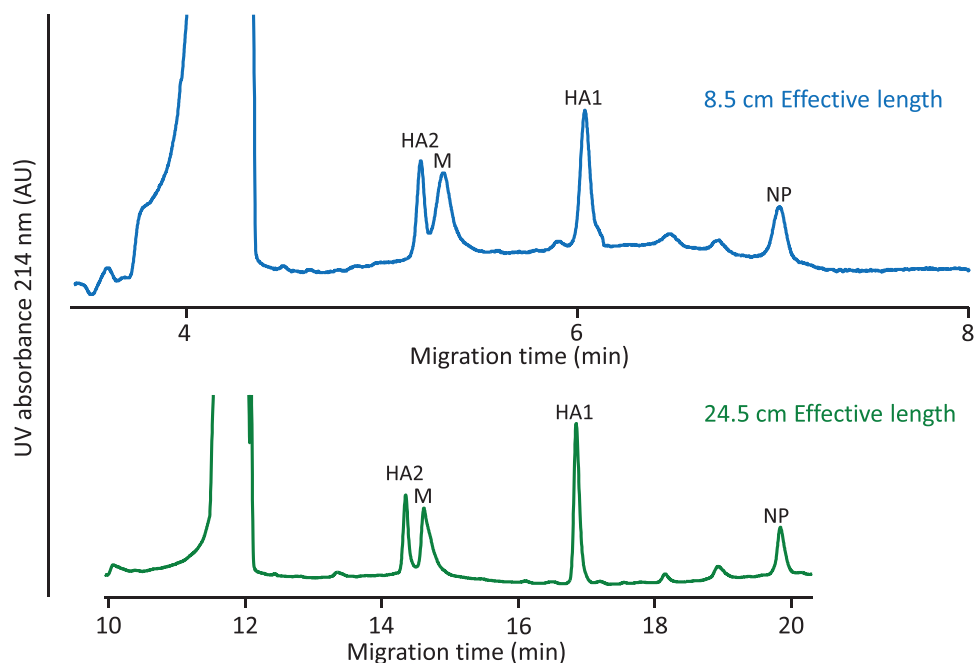


Figure 2. Electropherogram results of influenza reference standard NIBSC B/Brisbane/60/2008 analyzed with CGE with an effective length of 24.5 cm or 8.5 cm, and peaks Hemagglutinin subunit 1 (HA1), hemagglutinin subunit 2 (HA2), matrix protein (M), and nuclear protein (NP). For other conditions, see text.

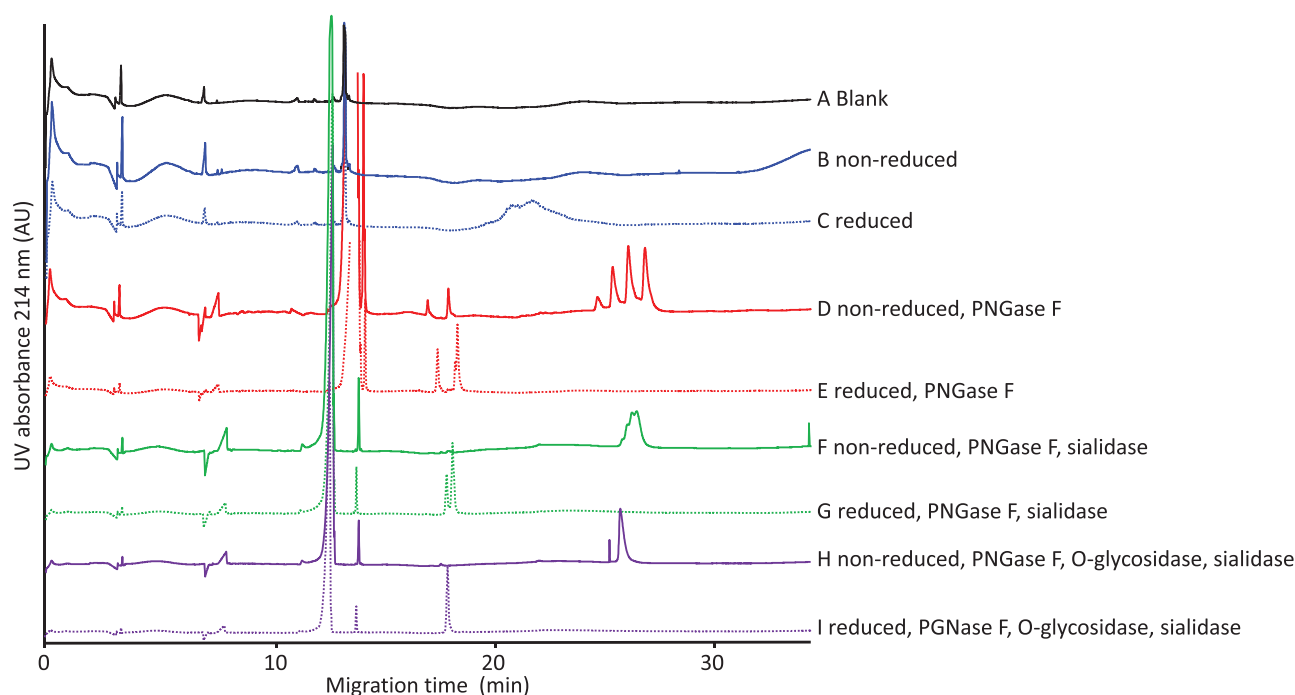


Figure 3. Effects of reduction and different deglycosylation protocols on the CE-SDS separation of a purified mini-HA sample, resulting in a glycan distribution overview of the protein. For experimental conditions, see text.

were also observed when the protein was reduced before PNGase F treatment (Figure 3E) and were likely monomer mini-HA with either 0 or 1 O-glycan attached. Sialidase treatment removed the sialic acids. Hence, a combination of PNGase F and Sialidase was expected to provide one peak. Nevertheless, multiple peaks were observed after PNGase F and Sialidase treatment under non-reduced (Figure 3F) or reduced

(Figure 3G) conditions, which was thought to be the effect of the heterogeneity of the remaining O-glycans after removal of sialic acid. After Sialidase treatment, later migration times were observed which could be explained by the removed sialic acids decreasing the number of negative charges of the glycoprotein. After PNGase F, Sialidase, and O-glycosidase treatment, all glycans were removed and one peak for the gly-

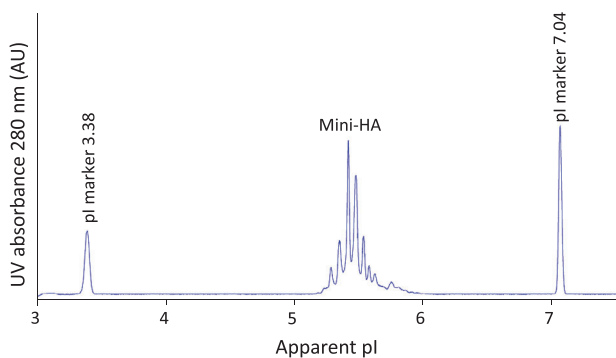


Figure 4. Typical electropherogram of a purified mini-HA sample with icIEF. For experimental conditions, see text.

can free primary protein structure was observed, which was trimeric for the non-reduced (Figure 3H), and monomeric for the reduced (Figure 3I) sample.

The different sample treatments revealed that the heterogeneity of the sample was caused by different features of the glycans attached. Different sample treatments resulted in different peak profiles characterizing the protein PTMs (e.g., disulfide integrity, glycan profiling, sialic acid loading). Studying glycans in this way does not yield in-depth characterization of the location and building blocks, as could possibly be determined by peptide mapping LC-MS [75,76], and the glycan derivatization assays like the CE-LIF application [77], and UPLC-LIF application [78]. Nonetheless, CE-SDS peak profiling provided an overview of the overall distribution of glycans on the mini-HA protein with different sample preparation and could be a quick high-throughput check for protein PTM quality, see Table 1 application 5.

3.3.3 Mini-HA Charge purity

A cIEF method was designed to determine the purity of mini-HA based on charge, in addition to the size-based CE-SDS method. The charge of proteins is affected by various factors such as amino acid composition, pH, and PTMs. Protein charge can be analyzed by several techniques such as cIEF [79], icIEF [80], CZE, and IEC. All of these techniques have the potential to separate the different charge species, the optimal technique might vary per protein. Both CZE and IEC methods have a lot of critical method parameters (CMPs) to be developed, e.g., capillaries, columns, buffers, etc., complicating method development. cIEF is more complex and has longer run times compared to icIEF due to the need of mobilization after focusing. The icIEF CMPs, such as the type and concentration of ampholytes, spacers, and sample diluent additives (e.g., urea, guanidine, etc.), could easily be optimized. Therefore, the icIEF application was selected, developed, and validated, see Table 1 application 6 and Figure 4. It should be noted that an apparent *pI* was determined and not a true *pI* for the same reason as for all other IEF methods (effect of sample treatment and separation conditions on the folding

and PTMs and thus the net charge of the protein), and the ampholyte gradient being pseudo-linear [81,82].

3.3.4 Mini-HA Stability

Both the CE-SDS and the icIEF methods for mini-HA purity determination were used to study mini-HA degradation. Several stressed conditions (i.e., thermal stress (70°C and 95°C), basic stress, and chemical oxidative stress) were applied for 24 h and thereafter the samples were analyzed with the CE-SDS and icIEF methods and compared to the 24 h at RT control sample. The CE-SDS method was used to determine size changes, such as hydrolysis. The icIEF method was expected to be sensitive for PTMs changing the *pI* of the desialized mini-HA (e.g., disulfide-scrambling, deamidation, oxidation, isomerization, hydrolysis).

The main mini-HA peak area decreased, and the % peak area with migration times earlier than the main peak increased for all stressed samples determined with CE-SDS, see Table 2 and Figure 5A. The %peak area with migration times later than the main peak was increased after 24 h at 95°C and after 24 h in basic conditions, see Table 2. Peaks migrating earlier than the main peak were likely degraded mini-HA (e.g., hydrolyzed mini-HA), and the later migrating peaks were suggested to be larger mini-HA aggregates. However, analytical artifacts, such as the effect of stress conditions on the sample preparation efficiency, could not be excluded.

Very distinct *pI* ranges and profiles were determined with icIEF for each stressed condition, see Table 3 and Figure 5B. Incubation for 24 h at 70°C resulted in a narrow *pI* range and was thought to be caused by disulfide reduction, reducing trimers and possible dimers into monomers. Incubation for 24 h at 95°C resulted in an apparent *pI* shift to lower pH similar to basic conditions. The *pI* shift could be explained by deamidation, isomerization, and hydrolysis, which are related to pH and temperature stress. Oxidation increased the apparent *pI* compared to the control sample. The peaks were not identified at the time since peak identification in icIEF is challenging and applications like icIEF-MS [83,84] were not at hand.

It is important to note that the icIEF peak % areas were not used for degradation pathway analysis, since the apparent *pI*s of the peaks were significantly different and could not be correlated between conditions.

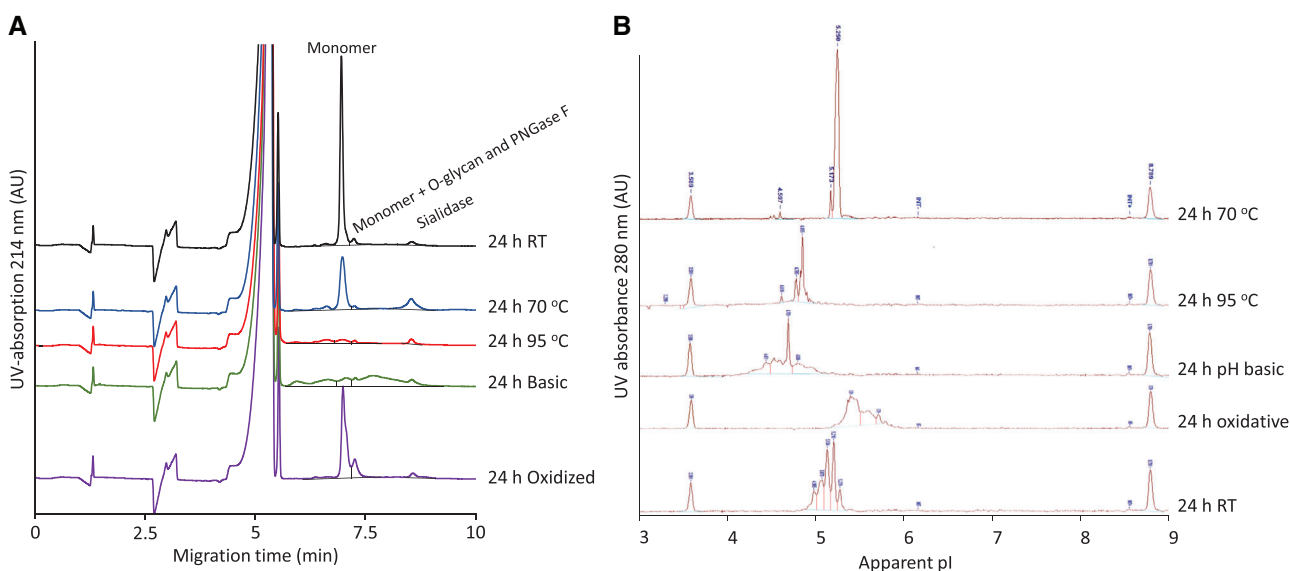
Due to the precision and the stability-indicating power of both methods, the methods were used to identify possible routes of degradation supporting an early product CQA analysis and future product quality and comparability assessments.

3.4 Sabin inactivated polio vaccine

Another example of using CE-SDS for viral protein analysis was for the development of a Sabin inactivated trivalent polio vaccine (sIPV). The identity of each serotype was to be

Table 2. Effects of several stressed conditions on a purified mini-HA sample analyzed with CE-SDS on the main peak corrected area recovery compared to the 24 h RT sample and the percentage of the main peak, low molecular weight (LMW), and high molecular weight (HMW) species

Condition	Deglycosylated mini-HA monomer [% recovery]	Deglycosylated mini-HA monomer [% Area]	LMW [% Area]	HMW [% Area]
24 h RT	100%	96.7%	2.6%	0.7%
24 h 70°C	51%	89.1%	10.9%	0.0%
24 h 95°C	5%	10.0%	86.1%	3.9%
24 h pH Basic	46%	21.3%	70.4%	8.3%
24 h pH Oxidized	73%	96.8%	2.0%	1.3%

**Figure 5.** Effects of several stressed conditions on a purified mini-HA sample analyzed with (A) CE-SDS and (B) icIEF. For experimental conditions, see text.**Table 3.** Effects of several stressed conditions on a purified mini-HA sample, analyzed with icIEF

Condition	Main peak apparent pI [pH]	Apparent pI range [pH]
24 h RT	5.13	4.99–5.28
24 h 70°C	5.25	5.17–5.25
24 h 95°C	4.85	4.62–4.85
24 h pH basic	4.81	4.45–4.81
24 h pH oxidative	5.39	5.39–5.71

confirmed by analytical testing. Immunochemical methodologies, like antibody-mediated viral neutralization assays, SRID assays, or D-antigen determination with ELISA, are commonly used for virus type identification [85–88]. All these methodologies use antibodies for specific detection of the virus subtype. Antibodies are very specific, but are also costly to develop, to produce, and to control the quality of. A four-step approach was used to optimize a CE-SDS method to

identify poliovirus types based on protein profiles as an alternative non-antibody method. Due to this four-step approach, an sIPV identity method was developed in 4 days, see Table 1 application 7 and [34].

3.5 Adenovirus vector vaccine

The previously discussed vaccines are examples of attenuated, inactivated, or subunit vaccines. Another type of vaccines are the viral vector vaccines, where a safe virus is used as a carrier for a pathogenic gene in order to elicit a specific antigen immune response. Adenoviruses are a type of viruses used as viral vector vaccines, currently for example to combat COVID-19 [89] and Ebola [90]. Adenoviruses are non-enveloped common cold viruses with a diameter of about 90 nm. Double-stranded DNA is encapsidated by proteins and about 13 different types of proteins are present in the virion [91]. The individual proteins can be separated by UPLC [53]. The adenovirus vector vaccines are produced in bioreactors with cultured human

cells by adenovirus vector seed inoculation (e.g., HEK293, Per.C6®) [19,92–103]. Purification of the adenovirus can be performed via cell lysis, clarification of the adenovirus particles from the cell debris and host cell DNA (HC DNA), AEX-filtration, and UF/DF [19,92,95,104–109]. After purification, the adenovirus vaccines are formulated and packaged before storage, distribution, and clinical usage [110–116]. See Supporting Information Section 2 for a detailed process overview. Different CQAs and CPPs are important in the CS of each of these steps. Several examples are provided for the use of CE to determine these CQAs per process step.

3.5.1 Seed production

For bioreactor inoculation, a precise and accurate seed adenovirus concentration was needed. Previously, an adenovirus particle content CZE method for in-process control testing (IPC) of drug substance production was developed and validated [19,20], see Table 1 application 11. The development took experience from other large biomolecule and viral analysis CZE methods into account [9,13,15–18,21–27,30,117,118]. However, in the literature mostly BFS capillaries in combination with borate buffers and SDS were used. This is not appropriate for adenovirus particles, as SDS denatures and disintegrates the adenovirus particle, and the adenovirus particle adsorbs to BFS. Therefore, a neutrally polyvinyl alcohol (PVA) coated capillary in combination with a Tris-tricine buffer and polysorbate-20 BGE were used for adenovirus analysis with CZE. Downstream process samples can be analyzed without sample pretreatment, but for crude samples from the upstream process, DNA-related interference peaks and spikes were observed. With the addition of a cell lysis and a DNase sample pretreatment [19], the interference with the adenovirus concentration determination was reduced and this method was validated for seed release testing, see Table 1 application 8. See van Tricht, et al. for method details [19].

3.5.2 Cell lysis

The adenovirus purification process was designed with a detergent lysis step after adenovirus production to release the virus from the host cells and limit the host cell DNA and host cell protein (HCP) release. However, the detergent used was put on Annex XIV by the EU REACH-Committee as the degradation product was deemed environmentally hazardous and will, therefore, need to be replaced. Alternative lysing agents were studied for their effect on adenovirus yield, and HCP and HC DNA release. The number of analytical methods that can cope with complex matrices such as cell lysates without extensive sample prep is limited. However, the CZE method showed to be precise and accurate for a complex sample matrix such as clarified harvest (CH) ([19, 20], Table 1 application 12). Therefore, CZE was used to determine the Ad26

concentration, and to study the impact of the detergent on other peaks in the electropherogram that are related to HC DNA, HCP, cell components, or aggregates.

In general, the peak profiles, i.e., separation and peak shapes obtained after lysis with different detergents, were comparable, see Figure 6. No new peaks were observed that could be associated with excessive HC DNA, HCP, cell components, and aggregates. This suggested that each of these detergents performed equivalently. Subsequently, the CZE method was used during hold time studies to select the most optimal lysis agent and lysis conditions.

3.5.3 Clarification

Cell lysis is followed by HC DNA clarification. HC DNA content and size are safety CQAs due to potential infectiveness and oncogenic properties [119–122]. Therefore, regulatory authorities expect a CS to limit the HC DNA presence in vaccine products to 10 ng/dose for continuous cell lines and a median size of ≤ 200 bp [123–125]. The CS consisted of i) removal of DNA via detergent aided DNA precipitation with domiphen bromide (DB) [19,20,95] and ii) testing of HC DNA content and fragment size distribution throughout the vaccine production process.

Host cell DNA analysis

An HC DNA fragment size determination method was needed with an LOD of 10 ng/dose. First, four different DNA extraction methods were evaluated. The Wako DNA Extractor® kit [50] in combination with an RNase treatment was determined to be the best extraction method due to high DNA recoveries, high throughput, and short extraction time, and was deemed easiest to transfer to other testing sites. Second, for DNA fragment separation and detection, the Sciex eCAP DNA 1000 application was evaluated, see Table 1 application 13. Three pronounced bands were observed below 200 bp for the clarified harvest and AEX-filtrate with the slab-gel *Electrophoresis* (Figure 7A) and corresponded with the determined peak patterns with the Sciex eCAP DNA 1000 application (Figure 7B). The large band at > 1000 bp with slab-gel *Electrophoresis* is Ad26 intact DNA, and out of scope for this method. Noteworthy, for the Sciex eCAP DNA 1000 application the samples were diluted to have the same adenovirus concentration, which is not performed for the slab-gel electrophoresis. The reason for this is that a too high Ad26 DNA concentration disturbed the electrophoresis. This effect could have been the reason for the observed spikes at > 25 min in this electropherogram. A similar decrease in < 200 bp fragments was observed with the slab-gel electrophoresis and the Sciex eCAP DNA 1000 application and were deemed interchangeable for this purpose.

Nonetheless, The eCAP DNA 1000 application took 3–4 h to prepare and analysis times were 35 min per sample, whereas the slab-gel application, with the usage of Flash Gels,

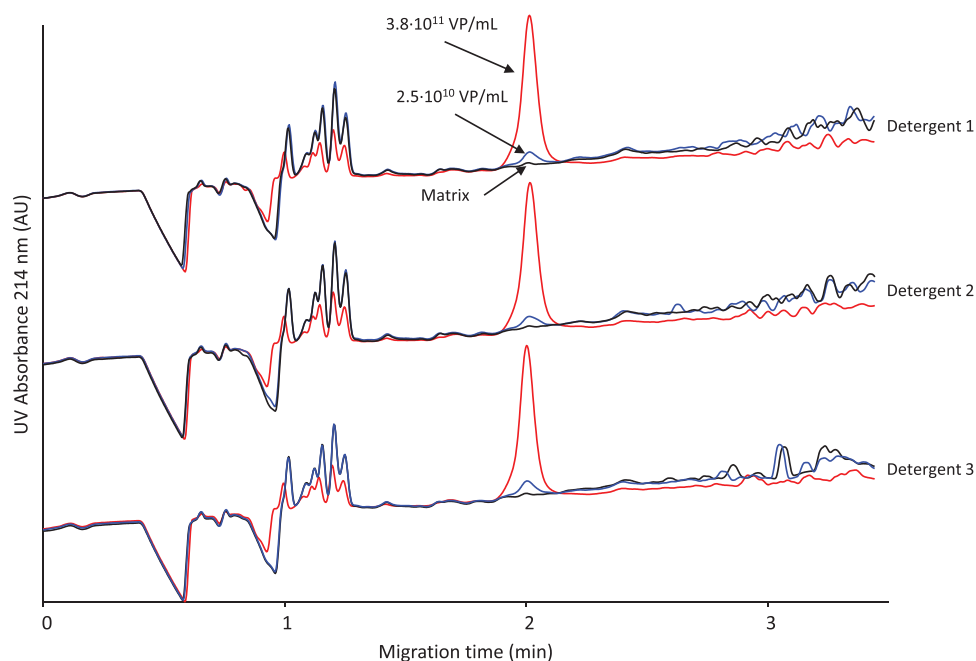


Figure 6. Effects of three different cell lysis detergents at 0, 2.5×10^{10} , and 3.8×10^{11} VP/mL on the Ad26 concentration determination and impurities with CZE. The 3.8×10^{11} VP/mL sample was diluted in FB to fit the CZE method range. The matrix was obtained from the supernatant after centrifugation at 20,000 rcf and 4°C for 1 h. For other conditions, see text.

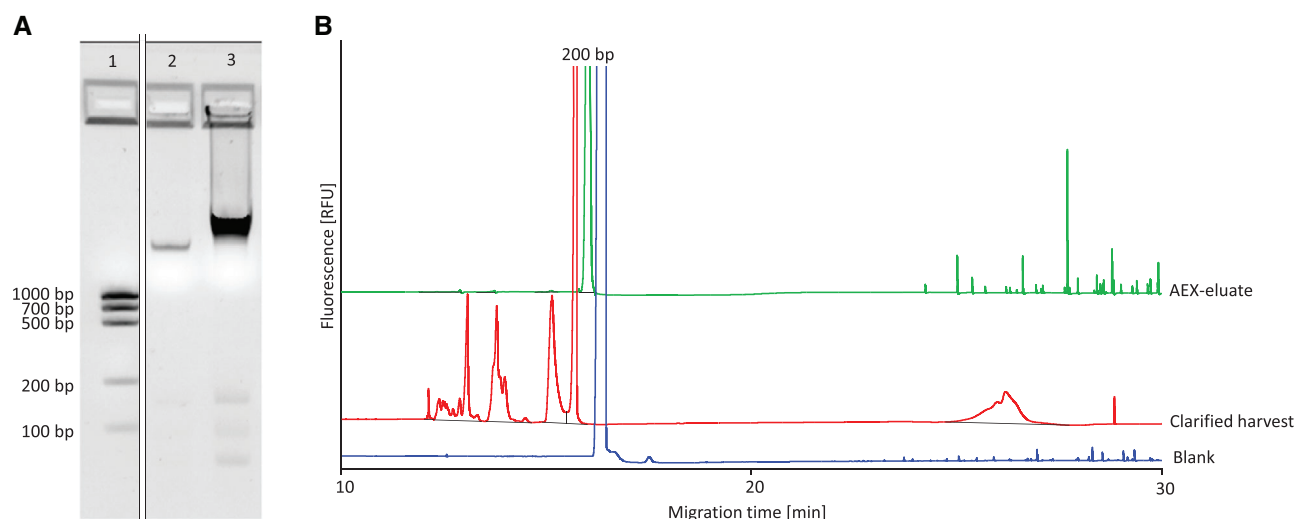


Figure 7. Example in-process samples analyzed with (A) slab-gel electrophoresis in lane 1 the DNA QuantLadder 100–1000 bp, lane 2 clarified harvest and lane 3 AEX-eluate, and (B) CGE eCAP 1000 application of blank (Blue), the clarified harvest (red), and the AEX-eluate (green). The DNA ladder, and two samples were ran on the same slab-gel and irrelevant lanes were removed by picture splicing indicating with a separator line in the figure. For experimental conditions, see text.

could be prepared in 10 min and 11 samples were analyzed simultaneously in 5 min. In addition, the slab-gel application was perceived to be less labor intensive, and to require less training.

Domiphen-adenovirus interaction

Domiphen is a cationic detergent that is added during clarification to precipitate the negatively charged HC DNA. The domiphen concentration is a CPP [95] and a sub-optimal concentration leads to ineffective DNA clearance, AEX-filter

blockage, or low adenovirus yields. Other CPPs that have an impact on the domiphen-HC DNA interaction are the clarification incubation time and temperature, adenovirus concentration, ionic strength, and pH. Domiphen does not only interact with DNA, but also with other negatively charged components like the adenovirus particle. This has a potential impact on the affinity of the adenovirus particles for the AEX filter and on the CZE analysis for adenovirus concentration determination. To set PARs for the clarification, the effect of the domiphen concentration on the adenovirus particle was studied.

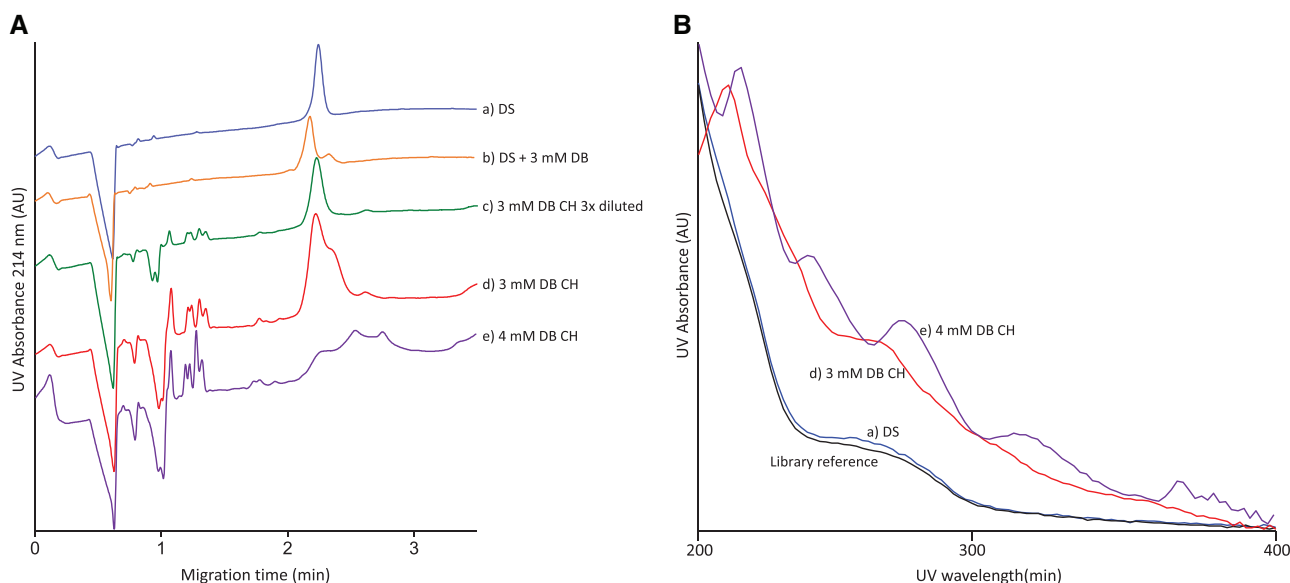


Figure 8. Effect of different concentrations of Ad26. In (A) CZE electropherograms with (a) DS, (b) DS with 3 mM DB added, (c) a 3 mM clarified harvest (CH) diluted with DS FB, (d) a 3 mM CH, and (e) a 4 mM CH, and (B) the respective Ad26 peak spectra of the library reference (black), (a) DS sample, and (d) 3 mM DB CH and (e) 4 mM DB CH. For experimental conditions, see text.

Clarification was originally performed at 3 mM DB (Figure 8A d)), and an additional later migrating adenovirus peak shoulder was observed in CH compared to a DS sample (Figure 8A a)) with CZE. Spiking of the 3 mM DB into the DS sample (Figure 8A b)) had a similar effect. The later migration time of the shoulder indicate lower electrophoretic mobility, so a lower charge/size ratio. This means that the Ad26 particle is larger, or less charged, or a combination of the two. Both a larger particle and a lower surface charge can be the result of an interaction of domiphen with adenovirus. DLS analysis confirmed that the hydrodynamic radius of Ad26 increased from 90–100 nm to 100–110 nm after DB addition to DS. The Ad26 peak ultra-violet (UV) spectrum also changed and indicated more scattering and thus larger particles (Figure 8B).

During further Ad26 AEX-filtration purification no yield loss was observed at 3 mM DB and no domiphen could be determined in the AEX-filtration sample with RP-HPLC with charged aerosol detection. Dilution of the CH sample with FB of the DS (Figure 8A c)) resulted in a narrow single peak. Both results indicate that the domiphen-adenovirus interaction is reversible, and that adenovirus is cleared from domiphen during AEX processing.

The Ad26 particle yield significantly decreased when clarification was done with 4 mM DB (Figure 8A e)) instead of 3 mM DB (Figure 8A d)). With CZE, the CH with 4 mM DB resulted in a broad pattern (2–3 min) with several peaks, indicating a very heterogeneous pool of adenovirus particles. With DLS, hydrodynamic radii of 500–1000 nm were observed in the CH samples containing 4 mM DB, compared to 90–100 nm for DS samples. Therefore, it is likely that clarification with 4 mM DB resulted in Ad26 particle aggregates which were lost in the process, possibly due to precipitation or a decreased

affinity for the AEX-filter. The adenovirus pattern UV spectra were comparable to the 3 mM DB CH, suggesting scattering and thus larger particles.

Interestingly, re-injection of clarified samples after 24 h resulted in decreased Ad26 concentrations and the decrease was more pronounced with longer hold times and higher DB clarification concentrations. Clarification duration studies indicated that the Ad26 yield decreased rapidly with time and timely process continuation was essential. The use of CZE reduced analysis times and process hold times from approximately three days to less than 2 h, because of the combined effect of faster analysis and higher precision. Consequently, a fast, accurate, precise, and robust at-line assay for IPC testing was validated [20], and implemented at different sites, see Table 1 application 9. The observed shoulder with high DB concentration did not impact the method performance. Subsequently, the CZE method was used to set PARs for a robust and consistent adenovirus purification process, and the target DB concentration for clarification was set to a maximum value.

Bromide content

HC DNA Clearance with domiphen is performed by adding domiphen bromide to the bulk solution. As bromide is known to be an anticonvulsant and sedative, an acceptance limit of not more than 4 µg/dose for the adenovirus vaccine product was determined. During the purification process, bromide is cleared to well below this limit. A CZE method based on the CZE method from Ståhlberg et al. [47] was developed to determine the bromide concentration during the purification process to prove bromide clearance. Bromide and chloride are among the fastest migration anions that result

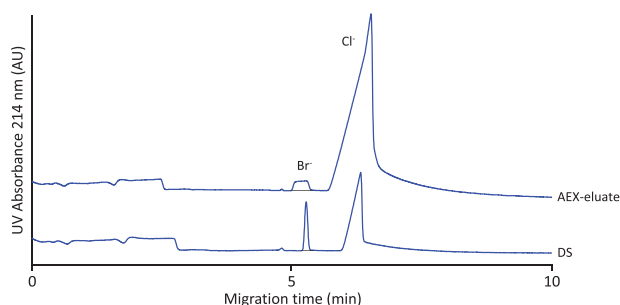


Figure 9. Bromide (8 $\mu\text{g/mL}$) spiked into AEX-eluate and DS samples and analyzed with CZE. For experimental conditions, see text.

in a method free of interference of matrix components. The method also makes use of the absorbance of bromide at low UV-wavelengths in order to avoid the need for indirect detection methods.

Although chloride has low UV-absorbance, high sample chloride concentrations could cause loss of separation between the bromide and chloride peak due to electromigration dispersion. Both the addition of iodide as leading electrolyte and milli-Q water sample dilution were tested to improve the peak efficiency and decrease electromigration dispersion by influencing the transient isotachopheresis mechanism. Dilution with milli-Q water improved the separation sufficiently, see Figure 9. Still, a squared bromide peak was observed for the sample with high chloride concentration, but despite the peak shape, the method was fit for purpose and was validated, see Table 1 application 14.

3.5.4 AEX-filtration and ultra- and diafiltration

After clarification, HCPs are removed during AEX-filtration and UF/DF is performed to reduce the concentration of remaining matrix components, and to formulate the adenovirus particles in a stable environment, resulting in so-called drug substance (DS).

Host cell Protein AEX-filter blockages

During the AEX-filtration process, the amount of material loaded on the AEX-filter is a CPP as overloading could result in yield loss or filter blockage, while underloading could result in yield loss due to adsorption.

In the example given in Figure 10A, (the front of) a new peak at 3.5 min was observed with CZE in cell lysed (LH 2) and clarified (CH 2) samples compared to the lysed harvest (LH 1) and clarified samples (CH 1) from a reference batch. The new peak did not interfere with the Ad26 determination, however, the appearance of this peak correlated with high AEX-filtration pressures. An absorbance maximum in the UV-spectrum at 280 nm suggested that the peak contained protein, see Figure 10B. Subsequently and as a result of this observation in the CZE determination, at-line analysis

was performed allowing for fast root-cause investigation and resolution of the issue.

Chloride content

During AEX-filtration, high concentrations of NaCl are used for adenovirus elution from the AEX-filter. In addition, NaCl is present in the vaccine product as a tonicity agent and is therefore considered a CQA. A NaCl concentration outside the intended range leads to unnecessary pain at the injection site and is associated with adenovirus instability [110–116]. For these reasons, the chloride concentrations were determined in the FB raw material, throughout the UF/DF, and in the final DS, for process characterization and process validation purposes. For process validation, a concentration determination with accuracy 95–105% and intermediate precision $\leq 5\%$ RSD was needed.

Several techniques could be considered to determine the chloride concentration. However, in the CZE method for Ad26 particle analysis, chloride is observed as an electromigration dispersed (triangular) indirect-UV peak in the migration time window 0.5–1.0 min. Therefore, we verified if the Ad26 CZE method could also be used for chloride quantification. This proved to be the case and the method was validated for Ad26 process validation as well as bed-site mixing studies of $\text{Al}(\text{OH})_3$ adjuvanted mini-HA, see Table 1 application 15 and Figure 11.

3.5.5 Drug substance and drug product

After UF/DF, drug substance is obtained and drug product can be produced. Both DS and DP are subjected to extensive testing for clinical release and stability testing. Important CQAs for release testing are the adenovirus identity, the product-related impurities such as empty and incomplete adenovirus particles, and the adenovirus concentration. For stability testing, it is important to determine the adenovirus concentration loss and to identify the route of degradation.

Strain identity

Adenovirus vaccines are common cold viruses and subtypes were selected to avoid pre-existing immunity toward the viral vector [126,127]. Different adenovirus subtypes can be produced in the same manufacturing facility or analyzed in the same lab. The different adenovirus subtypes have different physicochemical properties, e.g., pI, and amino acid composition [91]. A method that can discriminate selectively between different strains is a requirement. With the Ad26 CZE method, all tested different adenovirus subtypes were separated. Therefore, the method can be used for viral vector identity confirmation, see Figure 12. As CZE separation is based on charge/size ratio, the migration correlates to the number of negative charges on the adenovirus particle. The adenovirus particle surface charge determines the NaCl

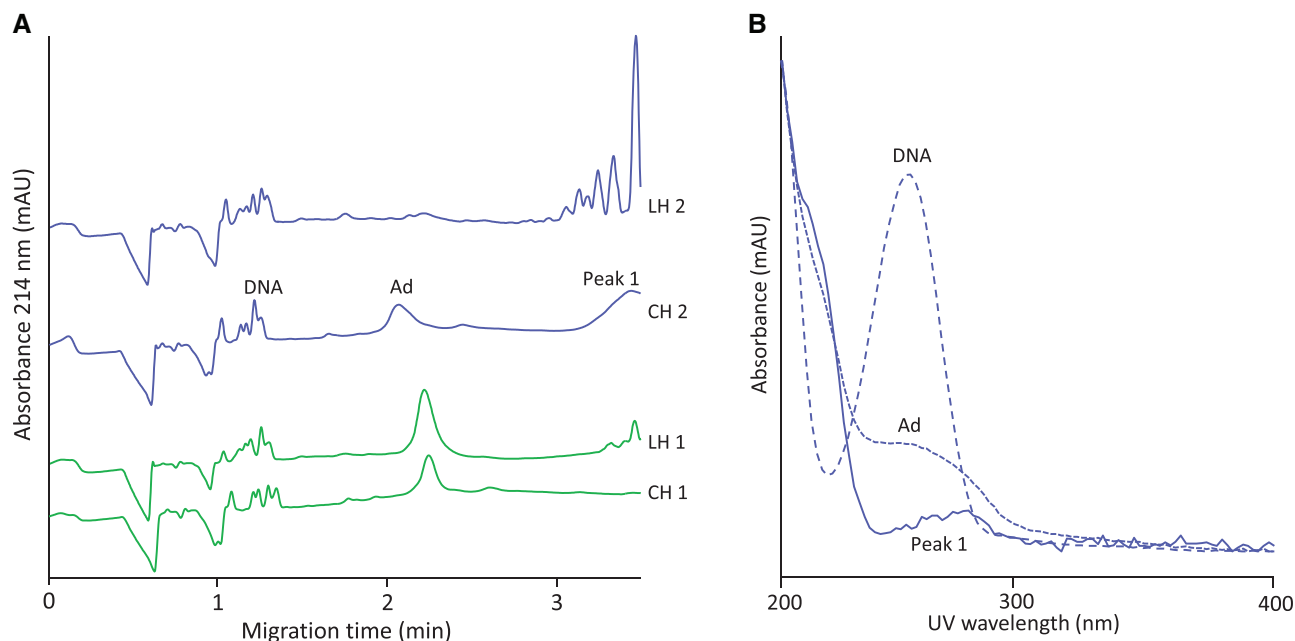


Figure 10. The front of a new peak observed in (A) electropherograms of lysed harvest (LH 2) and clarified harvest (CH 2) samples from a batch with AEX-filter blockage (blue), compared to lysed harvest (LH 1) and clarified harvest (CH 1) samples from a batch without AEX-filter blockage (green), analyzed with CZE, and (B) UV-spectra of annotated CH2 peaks. For experimental conditions, see text.

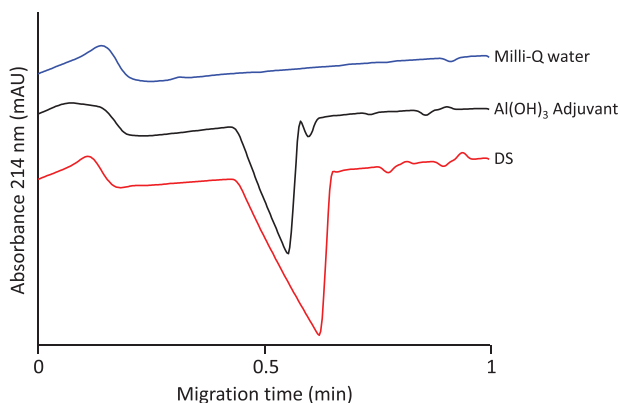


Figure 11. Chloride analysis of Milli-Q water, 50 mM NaCl added to aluminum hydroxide mini-HA (Al(OH)₃) adjuvant and purified Ad26 DS with CZE. Experimental conditions, see text.

concentration required during AEX-filtration, hence the CZE migration time is indicative of the NaCl concentration required for elution during AEX-filtration. For example, Ad35 migrated at 1.5 min and required a higher NaCl AEX-elution concentration than Ad26, which migrated at 2.1 min.

Adenovirus incomplete

During adenovirus production in the bioreactor, incomplete or empty particles are formed [128–131]. The concentrations of complete and incompletes can be determined by sedimentation velocity analytical ultra-centrifugation (SV-AUC) [132]. However, this method is elaborative, has low throughput, and

is expensive. Therefore, we tested whether we could determine the incomplete impurity percentage with the Ad26 particle CZE method. Incomplete and complete fractions were obtained with sedimentation equilibrium analytical ultracentrifugation (SE-AUC) in cesium chloride (CsCl) [128]. Viral particle concentrations were determined with CZE and fractions of incomplete and complete were mixed ranging from 0 to 100% incompletes.

Complete particles and incomplete virus particles were not separated, see Figure 13A. So, independent of having encapsidated DNA or not, the mobility of the virus particle is the same since the charge and the hydrodynamic size remain the same. UV-spectra and the optical density ratio at 260 nm and at 280 nm were significantly different from 0% incompletes at 50% incompletes, see Figure 13B. This is above the expected %-incompletes in DS and DP samples. Therefore, the relative number of incomplete particles could not be determined with the CZE method.

Content release testing

Adenovirus vector-based vaccines are dosed based on the vector particle concentration to avoid lack of efficacy or causing adverse effects [121,133]. OD260 [134,135] or quantitative polymerase chain reaction (qPCR) [136–139] have been used for adenovirus concentration determination. Van Tricht et al. reported an intermediate precision for qPCR of 15.9% RSD (or 8.1% RSD for 3 runs with 3 replicates per run) and CZE of 6.9% RSD [20]. Since CZE was more precise, the Ad26 CZE method was initially validated in the range of 5.0×10^{10} – 1.5×10^{11} VP/mL for DS and DP release testing,

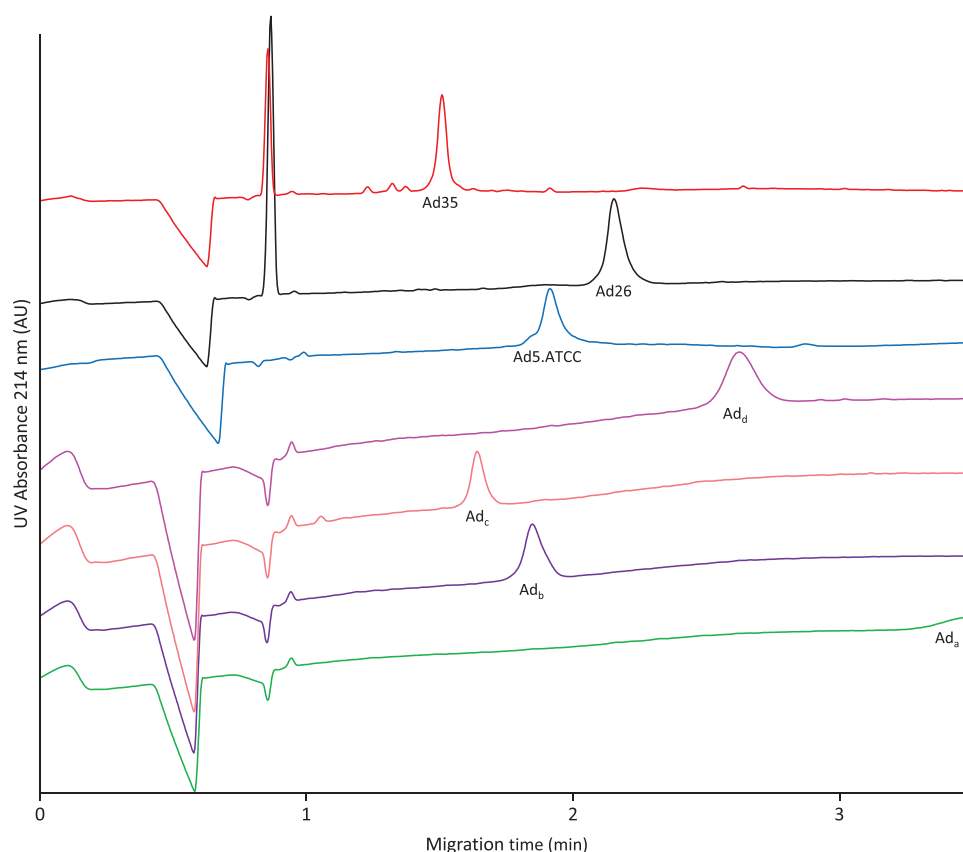


Figure 12. Electropherograms of different adenovirus subtypes analyzed with CZE, including human adenovirus 5 international reference standard Ad5.ATCC®[151]. For experimental conditions, see text.

see Table 1 application 10. In order to explore quantification of low-dose vaccines, additional sensitivity was needed.

A large-volume injection can be concentrated on-capillary based on a transient-ITP principle with chloride in the sample as leading electrolyte and tricine in the BGE as terminating electrolyte. In the Ad26 CZE method an injection of 1.4% of the capillary length was used. The transient-ITP principle provided the opportunity to increase the hydrodynamically injected sample volume to a maximum of approximately 50% of the capillary length. An LOD of 5×10^8 VP/mL (0.8 pmol/L) and an LOQ of 1.5×10^9 VP/mL (2.5 pmol/L) were readily achieved for DS and DP materials. A robust method was developed and validated for low-dose vaccines, with an injection volume of 25 s \times -100 mbar (approximately 14% of the capillary), see Table 1 application 16.

Stability testing

Product degradation causes loss of infectious adenovirus particles and formation of degradants, which could potentially impact both efficacy and safety of the product. Development of a stable vaccine DP could prevent product degradation and is best supported by studying product stability and the routes of degradation.

The DS and DP release testing method was also validated for stability testing, see Table 1 application 10. The stability-indicating power of the Ad26 CZE method was

validated by stressing a control sample at 50°C for 45 min (48% recovery compared to control), 50°C for 120 min (29% recovery compared to control), and 0.05% H₂O₂ for 24 h at RT (0% recovery compared to control). The method was used to study the effects of the formulation compositions and container types under different types of stress on the Ad26 particle stability. The FBs varied in buffer and salt types and concentrations with or without the presence of a preservative. The different vaccine FBs had no impact on the CZE method performance. Plastic and glass type containers were used, and the DP formulations were stored at 25°C during 7 or 90 days.

FB2 with the preservative (FB2+) resulted in the highest recoveries after 7 days at 25°C in both the glass and plastic containers, see Figure 14A. Formulations with the preservative resulted in higher recoveries than formulations without the preservative. Lower recoveries were observed for plastic compared to glass containers. In another study, incubation at 25°C for 90 days resulted in the loss of Ad26 in all formulations, see Figure 14B. Interestingly, for either formulations decreases in migration times that are linked to oxidation were observed after 90 days. FB2 was designed to prevent oxidation and showed the least migration time decrease. Hence, the CZE content method was successfully used to find optimal and stable DP conditions (FB2+) and provided additional information regarding Ad26 particle changes during stress testing.

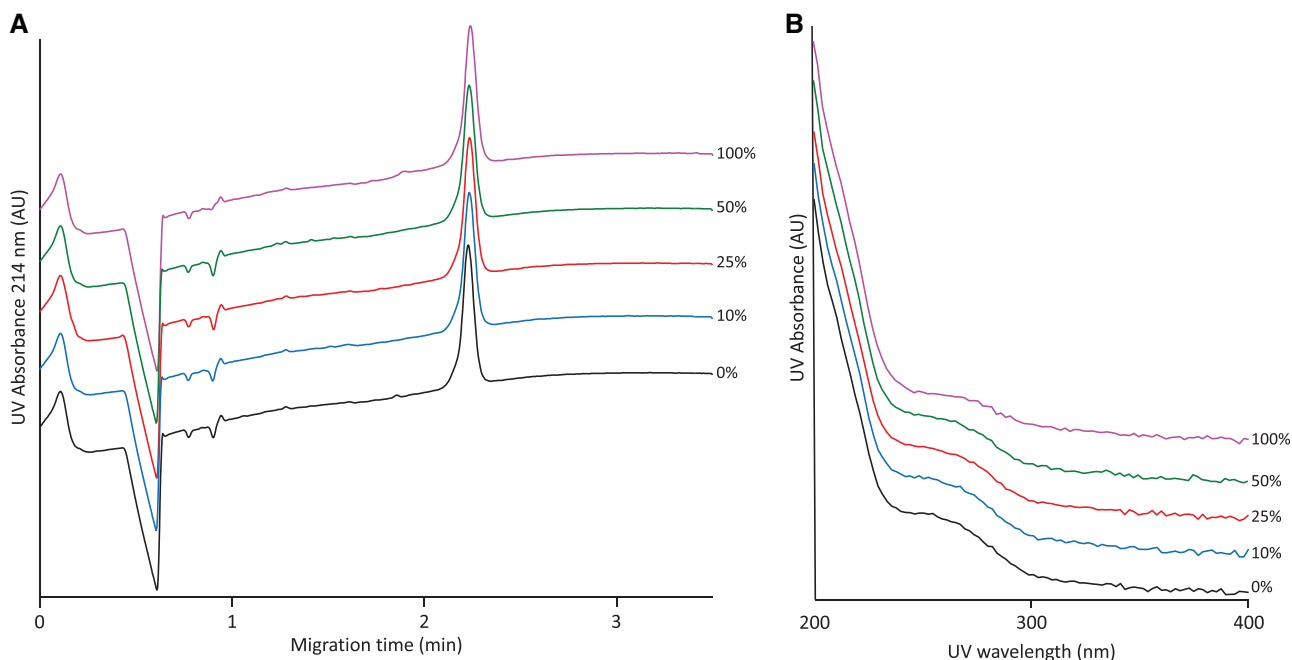


Figure 13. Effects of different fractions of incompletes at constant 214 nm UV absorbance analyzed with CZE, (A) electropherograms, and (B) UV-spectra of the Ad26 peak at 2.2 min. For experimental conditions, see text.

Concentration determination and adenovirus particle migration changes can be used to study the different routes of degradation, e.g., modification, aggregation, disintegration, and adsorption. Forced degradation studies were conducted to understand how Ad26 particles degraded and identify CQAs. Thermal stress (incubation at 50°C for 120 min or at 70°C for 45 min) and oxidation stress (incubation with 0.08% v:v H₂O₂ for 24 h or 0.40% v:v H₂O₂ for 17 h) were applied in this study example. The samples were analyzed with CZE [19], RP-HPLC [53], DLS, and ELS.

The CZE, RP-UHPLC, DLS, and ELS results for both oxidation conditions were similar, see Figure 15. The protein profiles for the oxidation conditions were different from the control sample, see Figure 15B. In RP-UHPLC, Protein II, the capsid protein hexon [91], shifted from 13.3 min in the control sample to 12.8 min after oxidative stress. The earlier retention time was most likely caused by a lower hydrophobicity due to adenoviral protein oxidation. The average hydrodynamic diameter was about 100 nm, comparable to the control sample, as expected from an intact non-aggregated

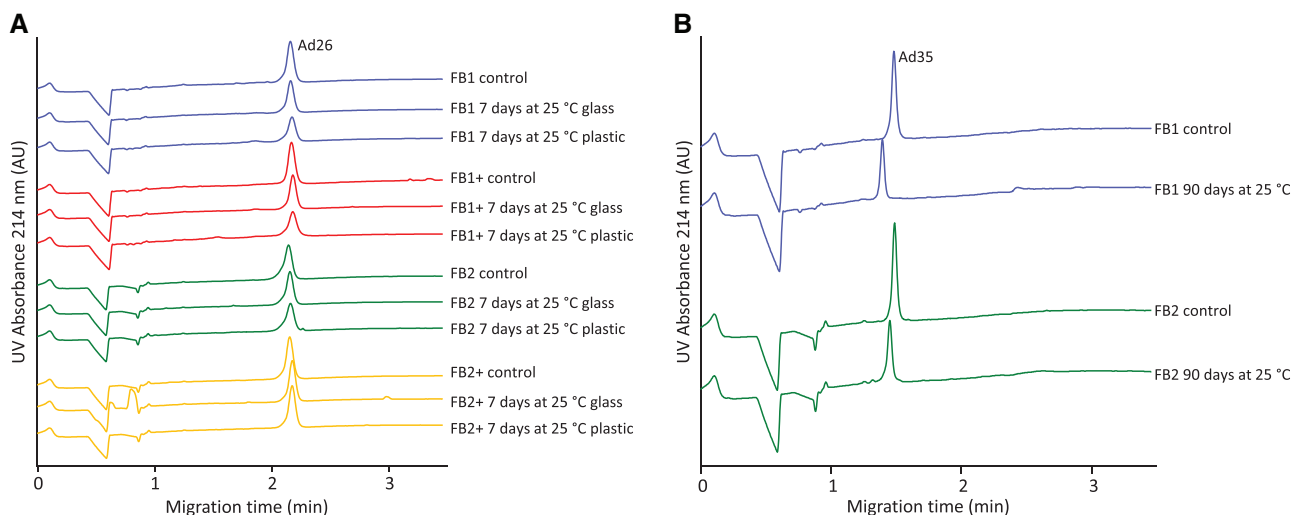


Figure 14. The effect of different FBs, some with preservative (+), analyzed with CZE after incubation in different containers (i.e., glass and plastic) at 25°C for, (A) 7 days, and (B) 90 days. For experimental conditions, see text.

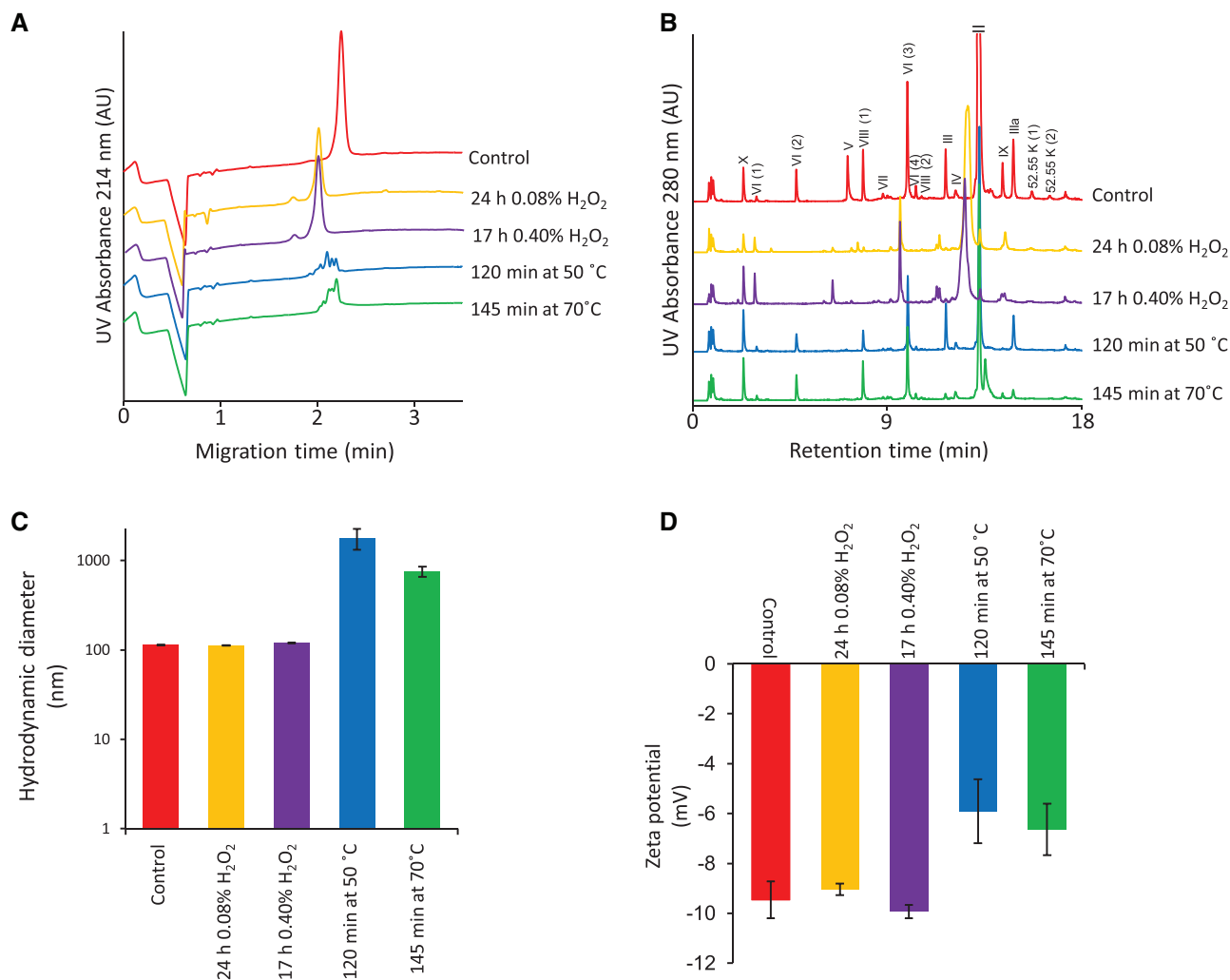


Figure 15. The effect of thermal stress 50°C 120 min (blue), and 70°C 45 min (green) and oxidation stress 0.08% w:v H₂O₂ for 24 h (yellow), and 0.40% w:v H₂O₂ for 24 h (purple) and a control sample (red), analyzed with (A) CZE, (B) RP-HPLC, (C) DLS, and (D) ELS. Experimental conditions, see text.

Ad26 particle, see Figure 15C. Nonetheless, higher polydispersity numbers (not presented) were found for oxidation stressed samples compared to the control, which suggested higher heterogeneity of particles diameters. In CZE, Ad26 peak at 2.2 min (control) was not detected in the oxidized samples, instead peaks at 2.0 min and 1.8 min were found, see Figure 15A. An earlier migration time indicates a smaller and/or more negatively charged particle. The peak at 2.0 min was identified as Ad26 and the peak at 1.8 min was suggested to be protein, based on the UV spectra (not presented). Ad26 particle destabilization and disintegration due to hydrophobicity decrease of hexon could result in free protein in the sample and higher particle diameter heterogeneity. The zeta potentials of the oxidized samples were similar to the control sample, suggesting that the average surface charge of the particles in the sample did not change, see Figure 15D. The hexon protein is much smaller than the Ad26 particle and could thus result in a higher electrophoretic mobility.

Differences were observed between the electropherograms (Figure 15A), hydrodynamic diameter (Figure 15C), and the zeta potential (Figure 15D) for the thermally stressed samples compared to the control sample, but not for the retention times for most of the Ad26 proteins (Figure 15B). In the electropherograms the main Ad26 peak was absent, and an earlier migrating cluster of peaks identified as aggregates (with UV spectrum, not presented) was observed. A higher hydrodynamic diameter was observed for the thermally stressed samples, also suggesting aggregation. The zeta potential was less negative for the thermally stressed samples compared to the control sample. This means that the average surface charge was less negative. A change in zeta potential could be caused by protein denaturation, followed by particle disintegration or aggregation. Aggregation cannot be detected with RP-HPLC due to the denaturing conditions applied to the sample before separation. Interestingly, the aggregates migration times were earlier and the total

corrected peak area was lower than for the adenovirus particles in the control samples. A later migration time was expected for aggregates of intact Ad26, due to the increase of size and the shielding of charge. The decrease in the area suggested components were not detected, which could be caused by precipitation, migration later than 3.5 min, or (unlikely) net positively charged aggregates migrating in the opposite direction. Disintegration of the Ad26 particle and aggregation of adenoviral protein with DNA could cause a heterogeneous pool of aggregates of different sizes and charges.

In total, the CZE results supported the interpretation of drug product stability and forced degradation studies, and determined CQAs, e.g., free in solution protein, on capsid protein, adenovirus melting, and aggregation temperature.

4 Concluding remarks

Although great results were obtained in using CE for vaccine analysis, similar challenges were encountered during the different application developments. A few are mentioned here.

Large biomolecules, such as proteins and viruses, are often heterogeneous due to PTMs or degradants. Large biomolecules are expected to result in more efficient peaks than small molecules due to the lower diffusion coefficients. However, broad adenovirus peaks were observed caused by the complexity and, therefore, heterogeneity of the adenovirus particle compared to for example a single protein virus-like particle [140,141]. In one example, glycans prevented the biomolecule from migrating through the gel buffer. Another frequent observation was aggregates/particulate matter in the form of spikes. Aggregates were possibly induced in the sample or in the capillary because of changing local environment due to, e.g., stacking or migration into the BGE. Sample treatment reduced the heterogeneity by removing PTMs, but could potentially cause a decreased stability of the analyte. Appropriate BGE selection can avoid degradation and aggregation of the sample and improve migration through the BGE.

Generally, ultra-pure or well-characterized standards are hardly available for viruses and vaccines. Because of the analyte heterogeneity in combination with the nanoliter sample volumes and the μL BGE volumes used in CE, peak identification by fraction collection in CE is challenging. BGEs, such as those used for the mentioned applications, are not compatible with other techniques such as MS and neither are complete viruses [16]. Nonetheless, great efforts are being made to develop applications with for example CE-SDS-MS and (i)CIEF-MS [142–147]. We used a combination of approaches for peak identification including the analysis of a selection of purified standards and blanks, physical removal of the component of interest, adding component-specific ligands (i.e., affinity capillary *Electrophoresis*), targeted component degradation, the use of highly specific detection (e.g., UV-spectra, intrinsic fluorescence or by staining, and others), and injection of characterized fractions collected with orthogonal techniques (e.g., ion-exchange chromatography, size exclusion chromatography, and others).

The use of high-grade chemicals and solution preparation best practices is important to improve assay ruggedness and robustness. Low-grade chemicals could potentially cause unwanted effects on the sample, such as degradation, aggregation, or adsorption, and have an impact on the BGE properties, such as ionic strength, viscosity, pH, etc., affecting the *Electrophoresis* separation. A new lot of any critical material needs to be verified before use, hence before the old lot runs out. Solution preparation best practices for capillary electrophoresis start with weighing in chemicals, instead of determining volumes or adjusting the pH or ionic strength manually. In addition, it is good practice to filter and/or sonicate solutions when chemicals are dissolved, or particles are to be expected. Reversed pipetting techniques could be beneficial in avoiding air bubble introduction during liquid transfer. The effects on pipetting accuracy of solution temperature, solution viscosity, and pipette tip adsorption should not be overlooked. If possible, ultra-sonication is a good practice to reduce air bubbles and undissolved particles.

Adsorption of biomolecules [148–150] and matrix effects [27] are well-known issues for the analysis of biomolecules, although often overlooked during method development. For CE applications, the analyte is only in contact with the capillary, not with any other parts of the instrument, limiting the type of surfaces to be dealt with. Adsorption was overcome during the adenovirus CZE method development by designing a BGE with low mobility, high ionic strength, high buffering capacity, and addition of a neutral surfactant in order to be robust for all process intermediates, within process variation and anticipated experimental process conditions, considering ionic strengths, pHs, viscosities, detergents, and DNA/protein content [19].

Sample preparation and stability are critical for biopharmaceutical applications, as the analytes are prone to degradation and aggregations, resulting in analytical artifacts. In addition, a solution that fits one biomolecule can be totally wrong for another one. Sample preparation and BGE and capillary selection for CE are often simplified by choosing an off-the-shelf standard application. However, the lack of fundamental method understanding of or knowledge about the composition of, for example, critical reagents, leads to robustness problems and sub-optimal assay conditions. Therefore, CMP effects need to be studied, and optimal methods to be designed, as demonstrated in [34].

For full control of methods, methods were designed and developed in-house. In general, there is a lot of uncertainty regarding the sample properties and the method parameter effects at the start of development. For some applications (not presented here), this uncertainty and complexity meant that a method could not be developed within the short time frame given. Having better knowledge of, e.g., physicochemical properties and sample stability, corroborates method development. Knowledge sharing among the CE community is key to overcome the method development threshold.

In our experience, designing a method from scratch, using the analytical quality by design (AQbD) principles, often resulted in a better method understanding and control,

and consequently led to a more robust and fit-for-purpose assay compared to off-the-shelf applications. In addition, fundamental technology understanding also provided the opportunity to use the method beyond the initial method scope, like the antibody CE-SDS application used for viral vaccine protein analysis such as (i) seasonal influenza HA quantification, (ii) universal mini-HA primary structure purity determination, (iii) polio protein identification, usage of the mini-HA primary structure CE-SDS method for (iv) glycan analysis, the Ad26 IPC CZE method that could be used for (v) all process intermediates, (vi) stability studies, (vii) product characterization, (viii) identification of additional protein in the context of AEX-filter blockage, (ix) domiphen adenovirus particle interaction studies, (x) low adenovirus concentration products, and the adenovirus content CZE method that could be used for (xi) chloride quantification.

In the end, however, the analytical test is as good as its user. Therefore, not only robust method design, but also operator training is of utmost importance. In our experience with method transfers, the normally expected and anticipated trainings are often analytical test procedure trainings only. Consequently, operators were not able to oversee and understand the consequences of habitual behaviors (e.g., local habits, and habits based on other technologies such as HPLC). Habitual behaviors were often overlooked during trainings and lead to method issues and difficult troubleshooting, especially in non-travel pandemic situations. We emphasize the importance of a holistic view on training and to include teaching the fundamentals of CE, the specific CE instrument, and the software, including the best practices for each. The test procedure is then the last step in the training. This approach, in combination with a sufficient number of trial runs, allows for building up experience and yields a decrease in the number of and time spend on troubleshooting. Eventually, it sets the basis for the operators to perform troubleshooting independently.

In total, the time we took to invest in understanding CE technology and develop applications resulted in a wide range of CE applications supporting viral vaccine analysis. CE took viral vaccine testing beyond what was previously possible and improved process and product understanding and, overall, the control of viral vaccine production with respect to safety, efficacy, and quality. Consequently, CE has become an indispensable asset to our analytical toolbox.

The authors thank Dr Martijn Schenning for the critical review of the manuscript, Martijn Kruger for data management, and Prof. Dr Hermann Wätzig for encouraging us to write this work.

The authors have declared no conflict of interest.

Data availability statement

The data that supports the findings of this study are available in the supplementary material of this article.

5 References

- [1] World Health Organization (WHO), *WHO Library Cataloguing-in-Publication Data*, ID: 978 92 4 150498 0, WHO, Geneva 2013.
- [2] European Medicines Agency (EMA), *ICH guideline Q8 (R2) on pharmaceutical development: Step 5*, ID: EMA/CHMP/ICH/167068/2004, EMA, London 2017.
- [3] U.S. Food and Drug Administration (USFDA), *Process Validation: General Principles and Practices*, ID: FDA-2008-D-0559, USFDA, Silver Spring, MD 2011.
- [4] European Medicines Agency (EMA), *ICH note for guidance on validation of analytical procedures: text and methodology*, ID: CPMP/ICH/381/95, EMA, London 1995.
- [5] Parenteral Drug Association (PDA), *PDA Technical Report No. 60–3 (TR 60–3) Process Validation: A Lifecycle Approach, Annex 2: Biopharmaceutical Drug Substances Manufacturing*, PDA, Bethesda, MD 2021 (ISBN: 9781945584244).
- [6] European Medicines Agency (EMA), *Guideline on process validation for finished products - information and data to be provided in regulatory submissions*, ID:EMA/CHMP/CVMP/QWP/BWP/70278/2012-Rev1,Corr.1, EMA, London 2016.
- [7] Yu, L. X., Amidon, G., Khan, M. A., Hoag, S. W., Polli, J., Raju, G. K., Woodcock, J., *AAPS J.* 2014, *16*, 771–783.
- [8] Hakemeyer, C., McKnight, N., st. John, R., Meier, S., Trexler-Schmidt, M., Kelley, B., Zettl, F., Puskeiler, R., Kleinjans, A., Lim, F., Wurth, C., *Biologicals* 2016, *44*, 306–318.
- [9] Kenndler, E., Blaas, D., *TrAC Trends Anal. Chem.* 2001, *20*, 543–551.
- [10] Kolivoška, V., Weiss, V. U., Kremser, L., Gaš, B., Blaas, D., Kenndler, E., *Electrophoresis* 2007, *28*, 4734–4740.
- [11] Kremser, L., Konecni, T., Blaas, D., Kenndler, E., *Anal. Chem.* 2004, *76*, 4175–4181.
- [12] Kremser, L., Okun, V. M., Nicodemou, A., Blaas, D., Kenndler, E., *Anal. Chem.* 2004, *76*, 882–887.
- [13] Kremser, L., Petsch, M., Blaas, D., Kenndler, E., *Anal. Chem.* 2004, *76*, 7360–7365.
- [14] Kremser, L., Petsch, M., Blaas, D., Kenndler, E., *Electrophoresis* 2006, *27*, 2630–2637.
- [15] Okun, V. M., Blaas, D., Kenndler, E., *Anal. Chem.* 1999, *71*, 4480–4485.
- [16] Okun, V. M., Ronacher, B., Blaas, D., Kenndler, E., *Anal. Chem.* 1999, *71*, 2028–2032.
- [17] Grossman, P. D., Soane, D. S., *Anal. Chem.* 1990, *62*, 1592–1596.
- [18] Hjertén, S., Elenbring, K., Kilár, F., Liao, J.-L., Chen, A. J. C., Siebert, C. J., Zhu, M.-D., *J. Chromatogr. A* 1987, *403*, 47–61.
- [19] van Tricht, E., Geurink, L., Backus, H., Germano, M., Somsen, G. W., Sängers-van de Griend, C. E., *Talanta* 2017, *166*, 8–14.
- [20] van Tricht, E., Geurink, L., Galindo Garre, F., Schenning, M., Backus, H., Germano, M., Somsen, G. W., Sängers-van de Griend, C. E., *Electrophoresis* 2019, *40*, 2277–2284.

- [21] Mann, B., Traina, J. A., Soderblom, C., Murakami, P. K., Lehmberg, E., Lee, D., Irving, J., Nestaas, E., Pungor, E., *J. Chromatogr. A* 2000, *895*, 329–337.
- [22] Halewyck, H., Oita, I., Thys, B., Dejaegher, B., Heyden, Y. V., Rombaut, B., *Electrophoresis* 2010, *31*, 3281–3287.
- [23] Oita, I., Halewyck, H., Pieters, S., Dejaegher, B., Thys, B., Rombaut, B., Heyden, Y. V., *J. Pharm. Biomed. Anal.* 2009, *50*, 655–663.
- [24] Oita, I., Halewyck, H., Pieters, S., Dejaegher, B., Thys, B., Rombaut, B., Heyden, Y. V., *J. Pharm. Biomed. Anal.* 2011, *55*, 135–145.
- [25] Oita, I., Halewyck, H., Pieters, S., Thys, B., Heyden, Y. V., Rombaut, B., *J. Virol. Methods* 2012, *185*, 7–17.
- [26] Oita, I., Halewyck, H., Thys, B., Rombaut, B., Heyden, Y. V., *J. Pharm. Biomed. Anal.* 2012, *71*, 79–88.
- [27] Oita, I., Halewyck, H., Thys, B., Rombaut, B., Heyden, Y. V., *Anal. Chim. Acta* 2012, *747*, 42–50.
- [28] Kolesar, J. M., Allen, P. G., Doran, C. M., *J. Chromatogr. B: Biomed. Sci. Appl.* 1997, *697*, 189–194.
- [29] Kolesar, J. M., Miller, J. A., Dhurandhar, N. V., Atkinson, R. L., *J. Chromatogr. B: Biomed. Sci. Appl.* 2000, *744*, 1–8.
- [30] Schnabel, U., Groiss, F., Blaas, D., Kenndler, E., *Anal. Chem.* 1996, *68*, 4300–4303.
- [31] Takátsy, A., Kilár, A., Kilár, F., Hjertén, S., *J. Sep. Sci.* 2006, *29*, 2802–2809.
- [32] Végyvári, A., Hjertén, S., *Electrophoresis* 2003, *24*, 3815–3820.
- [33] van Tricht, E., Geurink, L., Pajic, B., Nijenhuis, J., Backus, H., Germano, M., Somsen, G.W., Sängervan de Griend, C.E., *Talanta* 2015, *144*, 1030–1035.
- [34] Geurink, L., van Tricht, E., Dudink, J., Pajic, B., Sängervan de Griend, C. E., *Electrophoresis* 2021, *42*, 10–18.
- [35] Hamm, M., Ha, S., Rustandi, R. R., *Anal. Biochem.* 2015, *478*, 33–39.
- [36] Hamm, M., Wang, F., Rustandi, R. R., *Electrophoresis* 2015, *36*, 2687–2694.
- [37] Lancaster, C., Pristatsky, P., Hoang, V. M., Casimiro, D. R., Schwartz, R. M., Rustandi, R., Ha, S., *J. Chromatogr. B: Anal. Technol. Biomed. Life Sci.* 2016, *1032*, 218–223.
- [38] Rustandi, R. R., Anderson, C., Hamm, M., in: Beck, A. (Ed.), *Glycosylation Engineering of Biopharmaceuticals: Methods and Protocols*, Humana Press, Totowa, NJ 2013, pp. 181–197.
- [39] Rustandi, R. R., Loughney, J. W., Hamm, M., Hamm, C., Lancaster, C., Mach, A., Ha, S., *Electrophoresis* 2012, *33*, 2790–2797.
- [40] Rustandi, R. R., Wang, F., Hamm, C., Cuciniello, J. J., Marley, M. L., *Electrophoresis* 2014, *35*, 1072–1078.
- [41] Zhou, W., Tomer, K. B., Khaledi, M. G., *Anal. Biochem.* 2000, *284*, 334–341.
- [42] Guttman, M., Váradi, C., Lee, K. K., Guttman, A., *Electrophoresis* 2015, *36*, 1305–1313.
- [43] Tran, N. T., Taverna, M., Chevalier, M., Ferrier, D., *J. Chromatogr. A* 2000, *866*, 121–135.
- [44] Zhang, Z., Park, J., Barrett, H., Dooley, S., Davies, C., Verhagen, M. F., *Hum. Gene Ther.* 2021, *32*, 628–637.
- [45] Loughney, J. W., Lancaster, C., Ha, S., Rustandi, R. R., *Anal. Biochem.* 2014, *461*, 49–56.
- [46] Fabre, H., Blanchin, M. D., Bosc, N., *Anal. Chim. Acta* 1999, *381*, 29–37.
- [47] Stålborg, O., Sander, K., Sängervan de Griend, C., *J. Chromatogr. A* 2002, *977*, 265–275.
- [48] Nickerson, B., *J. Pharm. Biomed. Anal.* 1997, *15*, 965–971.
- [49] AB-Sciex, *IgG Purity and Heterogeneity Assay Kit: Application guide*, ID: RUO-IDV-05–6935-A, AB-Sciex, Framingham, MA 2018.
- [50] FUJIFILM Wako Chemicals U.S.A. Corporation, *DNA Extractor® Kit instructions*, ID: 1911KA2.
- [51] AB-Sciex, *dsDNA 1000 Kit: Application guide*, ID: RUO-IDV-05–11136-A, AB-Sciex, Framingham, MA 2020.
- [52] Bio-rad Laboratories, i., *ChemiDoc and ChemiDoc MP Imaging Systems with Image Lab Touch Software: User Guide*, ID: 10000062126 Ver E 2020.
- [53] van Tricht, E., de Raadt, P., Verwilligen, A., Schenning, M., Backus, H., Germano, M., Somsen, G. W., Sängervan de Griend, C. E., *J. Chromatogr. A* 2018, *1581–1582*, 25–32.
- [54] Nowak, C., Cheung, J., Dellatore, S., Katiyar, A., Bhat, R., Sun, J., Ponniah, G., Neill, A., Mason, B., Beck, A., Liu, H., *mAbs* 2017, *9*, 1217–1230.
- [55] European Medicines Agency (EMA), *Guideline on bioanalytical method validation*, ID: EMEA/CHMP/EWP/192217/2009 Rev. 1 Corr. 2, EMA, London 2011.
- [56] Lechner, A., Giorgetti, J., Gahoual, R., Beck, A., Leize, E., François, Y., *J. Chromatogr. B: Anal. Technol. Biomed. Life Sci.* 2019, *1122–1123*, 1–17.
- [57] Wang, X., An, Z., Luo, W., Xia, N., Zhao, Q., *Protein Cell* 2018, *9*, 74–85.
- [58] Leach, M. N. E., Carpick, B., *CASSS* 2018, CEP Pharm 2018.
- [59] Shala-Lawrence, A., Beheshti, S., Newman, E., Tang, M., Krylova, S.M., Leach, M., Carpick, B., Krylov, S.N., *Talanta* 2017, *175*, 273–279.
- [60] Li, T., Malik, M., Yowanto, H., Mollah, S., *Purity Analysis of Adeno-Associated Virus (AAV) Capsid Proteins using CE-SDS Method*, ID: RUO-MKT-02–9761-A, AB-Sciex, Framingham, MA 2019.
- [61] Zhang, C., Meagher, M.M., in: Phillips, T.M. (Ed.), *Clinical Applications of Capillary Electrophoresis: Methods and Protocols*, Springer, New York, New York, NY 2019, pp. 263–270.
- [62] Coudeville, L., Bailleux, F., Riche, B., Megas, F., Andre, P., Ecochard, R., *BMC Med. Res. Methodol.* 2010, *10*, 18.
- [63] Skehel, J., Wiley, D., *Annu. Rev. Biochem.* 2000, *69*, 531–569.
- [64] Su, B., Wurtzer, S., Rameix-Welti, M.-A., Dwyer, D., van der Werf, S., Naffakh, N., Clavel, F., Labrosse, B., *PLoS One* 2010, *4*, e8495.
- [65] Johansson, B. E., Bucher, D. J., Kilbourne, E. D., *J. Virol.* 1989, *63*, 1239–1246.
- [66] Neiryck, S., Deroo, T., Saelens, X., Vanlandschoot, P., Jou, W. M., Fiers, W., *Nat. Med.* 1999, *5*, 1157–1163.

- [67] Impagliazzo, A., Milder, F., Kuipers, H., Wagner, M. V., Zhu, X., Hoffman, R. M. B., van Meersbergen, R., Huizingh, J., Wanninger, P., Verspuij, J., de Man, M., Ding, Z., Apetri, A., Kükre, B., Sneekes-Vriese, E., Tomkiewicz, D., Laursen, N. S., Lee, P. S., Zakrzewska, A., Dekking, L., Tolboom, J., Tettero, L., van Meerten, S., Yu, W., Koudstaal, W., Goudsmit, J., Ward, A. B., Meijberg, W., Wilson, I. A., Radošević, K., *Science* 2015, **349**, 1301–1306.
- [68] van der Lubbe, J. E. M., Verspuij, J. W. A., Huizingh, J., Schmit-Tillemans, S. P. R., Tolboom, J. T. B. M., Dekking, L. E. H. A., Kwaks, T., Brandenburg, B., Meijberg, W., Zahn, R. C., Roozendaal, R., Kuipers, H., *Front. Immunol.* 2018, **9**, 2350–2350.
- [69] Impagliazzo, A., Meijberg, J. W., Radošević, K., Wagner, M., Ding, Z., US patent: US10117925B2 2015.
- [70] Milder, F. J., Ritschel, T., Brandenburg, B., Jongeneelen, M. A. C., Truan, D., Langedijk, J. P. M., *European patent: EP18152991* 2019.
- [71] Daniels, R., Kurowski, B., Johnson, A. E., Hebert, D. N., *Mol. Cell* 2003, **11**, 79–90.
- [72] Hebert, D. N., Zhang, J. X., Chen, W., Foellmer, B., Helenius, A., *J. Cell Biol.* 1997, **139**, 613–623.
- [73] Wang, A. L., Paciolla, M., Palmieri, M. J., Hao, G. G., *J. Pharm. Biomed. Anal.* 2020, **180**, 113006.
- [74] Scheller, C., Krebs, F., Wiesner, R., Wätzig, H., Oltmann-Norden, I., *Electrophoresis* 2021, **42**, 1521–1531.
- [75] Dotz, V., Haselberg, R., Shubhakar, A., Kozak, R. P., Falck, D., Rombouts, Y., Reusch, D., Somsen, G. W., Fernandes, D. L., Wührer, M., *TrAC Trends Anal. Chem.* 2015, **73**, 1–9.
- [76] Cipollo, J. F., Parsons, L. M., *Mass Spectrom. Rev.* 2020, **39**, 371–409.
- [77] AB-Sciex, *Fast Glycan Labeling and Analysis Kit: Application guide*, ID: RUO-IDV-05–4092-C, AB-Sciex, Framingham, MA 2020.
- [78] Scientific, T. F., *GlycanAssure™ HyPerformance APTS Kit: User guide*, ID: MAN0016959 2018.
- [79] AB-Sciex, *Beckman Coulter Capillary Isoelectric Focusing (cIEF) Analysis: Application guide*, ID: A78788AF, AB-Sciex, Framingham, MA 2014.
- [80] ProteinSimple, *User Guide for Maurice, Maurice C. and Maurice S.*, ID: P/N 046–, 295, ProteinSimple, San Jose, CA 2020.
- [81] Wu, J., Huang, T., *Electrophoresis* 2006, **27**, 3584–3590.
- [82] Demirdirek, B., Lan, W., Qiu, D., Ding, W., Iyer, L. K., Bolgar, M. S., Valente, J. J., *J. Chromatogr. B: Anal. Technol. Biomed. Life Sci.* 2019, **1105**, 156–163.
- [83] Chen, W., Kojtari, B., Satulovsky, J., Ostrowski, M. A., *Rapid and reproducible high-resolution charge variant analysis of adalimumab (mAb) using the IntaBio Imaged CIEF-MS System*, ID: RUO-MKT-02–13149, AB-Sciex, Framingham, MA 2021.
- [84] Chen, W., Ostrowski, M. A., Gupta, D., Gentalen, E., *Rapid, comprehensive, high resolution charge variant characterization using the IntaBio iCIEF-MS System with SCIEX TripleTOF 6600+ and Protein Metrics Byos Software*, ID: RUO-MKT-02–13150, AB-Sciex, Framingham, MA 2020.
- [85] Kouivaskaia, D., Puligedda, R. D., Dessain, S. K., Chumakov, K., *J. Virol. Methods* 2020, **276**, 113785.
- [86] Crawt, L., Atkinson, E., Tedcastle, A., Pegg, E., sIPV StudyGroup, Minor, P., Cooper, G., Rigsby, P., Martin, J., *J. Infect. Dis.* 2019, **221**, 544–552.
- [87] Minor, P. D., Ferguson, M., Evans, D. M. A., Almond, J. W., Icenogle, J. P., *J. Gen. Virol.* 1986, **67**, 1283–1291.
- [88] Rezapkin, G., Neverov, A., Cherkasova, E., Vidor, E., Sarafanov, A., Kouivaskaia, D., Dragunsky, E., Chumakov, K., *J. Virol. Methods* 2010, **169**, 322–331.
- [89] Mendonça, S. A., Lorincz, R., Boucher, P., Curiel, D. T., *NPJ Vaccines* 2021, **6**, 97.
- [90] Pollard, A. J., Launay, O., Lelievre, J. D., Lacabaratz, C., Grande, S., Goldstein, N., Robinson, C., Gaddah, A., Bockstal, V., Wiedemann, A., Leyssen, M., Luhn, K., Richert, L., Bétard, C., Gibani, M. M., Clutterbuck, E. A., Snape, M. D., Levy, Y., Douoguih, M., Thiebaut, R., *Lancet Infect. Dis.* 2021, **21**, 493–506.
- [91] Benevento, M., Di Palma, S., Snijder, J., Moyer, C. L., Reddy, V. S., Nemerow, G. R., Heck, A. J. R., *J. Biol. Chem.* 2014, **289**, 11421–11430.
- [92] Luitjens, A., van Herk, H., US patent: US2012031.5696A1 2012.
- [93] Berdichevsky, M., Gentile, M. P., Hughes, B., Meis, P., Peltier, J., Blumentals, I., Aunigs, J., Altaras, N. E., *Biotechnol. Prog.* 2008, **24**, 158–165.
- [94] Cortin, V., Thibault, J., Jacob, D., Garnier, A., *Biotechnol. Prog.* 2004, **20**, 858–863.
- [95] Goerke, A. R., To, B. C. S., Lee, A. L., Sagar, S. L., Konz, J. O., *Biotechnol. Bioeng.* 2005, **91**, 12–21.
- [96] Luitjens, A., Lewis, J. A., US patent: US10041049B2 2018.
- [97] Vogels, R., Bout, A., US patent: US7468181B2 2008.
- [98] Vogels, R., Havenga, M., Mehtali, M., US patent: US6492169B1 2002.
- [99] Weggeman, M., US patent: US6485958B2 2002.
- [100] Graham, F. L., Smiley, J., Russell, W. C., Nairn, R., *J. Gen. Virol.* 1977, **36**, 59–72.
- [101] Imler, J.-L., Mehtali, M., Pavirani, A., US patent: US6040174A 2000.
- [102] Massie, B., US patent: US5891690A 1999.
- [103] Kovesdi, I., Brough, D.E., McVey D.L., Bruder J.T., Lizonova, A., US patent: US5851806A 1998.
- [104] Weggeman, M., US patent: US67006405P 2013.
- [105] Weggeman, M., van Corven, E. J. J. M., US patent: US8124106B2 2012.
- [106] Konz, J. O. Jr., Lee, A. L., To, C. S. B., Goerke, A. R., US patent: US7326555B2 2008.
- [107] Carrión, M. E., Menger, M., Kovesdi, I., US patent: US6586226B2 2003.
- [108] Shabram, P. W., Giroux, D. D., Goudreau, A. M., Gregory, R. J., Horn, M. T., Huyghe, B. G., Liu, X., Nunnally, M. H., Sugarman, B. J., Sutjipto, S., *Hum. Gene Ther.* 1997, **8**, 453–465.
- [109] Tang, J. C.-T., Vellekamp, G., Bondoc, L. L. Jr., US patent: US6261823B1 2001.

- [110] Evans, R. K., Nawrocki, D. K., Isopi, L. A., Williams, D. M., Casimiro, D. R., Chin, S., Chen, M., Zhu, D. M., Shiver, J. W., Volkin, D. B., *J. Pharm. Sci.* 2004, **93**, 2458–2475.
- [111] Altaras, N. E., Aunins, J. G., Evans, R. K., Kamen, A., Konz, J. O., Wolf, J. J., *Adv. Biochem. Eng. Biotechnol.* 2005, **99**, 193–260.
- [112] Evans, R. K. Volken, D. B., Isopi, L. A., US patent: US7456009B2 2008.
- [113] Croyle, M. A., Cheng, X., Wilson, J. M., *Gene Ther.* 2001, **8**, 1281–1290.
- [114] Adriaansen, J., US patent: US9974737B2 2018.
- [115] Adriaansen, J., US patent: US20160199426A1 2016.
- [116] Sosnowski, B., Hoganson, D. K., Ma, J., Asato, L., Ong, M., Printz, M., Huyghe, B., D'Andrea, M., *BioProcessing J.* 2002, **1**, 43–48.
- [117] Mironov, G. G., Chechik, A. V., Ozer, R., Bell, J. C., Berezovski, M. V., *Anal. Chem.* 2011, **83**, 5431–5435.
- [118] Azizi, A., Mironov, G. G., Muharemagic, D., Wehbe, M., Bell, J. C., Berezovski, M. V., *Anal. Chem.* 2012, **84**, 9585–9591.
- [119] U.S. Food and Drug Administration (USFDA), *Characterization and Qualification of Cell Substrates and Other Biological Materials Used in the Production of Viral Vaccines for Infectious Disease Indications*, ID: FDA-2006-D-0223, USFDA, Silver Spring, MD 2010.
- [120] European Directorate for the Quality of Medicines & HealthCare (EDQM), *European Pharmacopoeia*, 5.2.3, ID: 01/2018:50203, EDQM, Strasbourg 2020.
- [121] European Directorate for the Quality of Medicines & HealthCare (EDQM), *European pharmacopoeia*, 5.14, ID: 01/2018:50203, EDQM, Strasbourg 2020.
- [122] Fallaux, F. J., Bout, A., van der Velde, I., van den Wollenberg, D. J., Hehir, K. M., Keegan, J., Auger, C., Cramer, S. J., van Ormondt, H., van der Eb, A. J., Valerio, D., Hoeben, R. C., *Hum. Gene Ther.* 1998, **9**, 1909–1917.
- [123] U.S. Food and Drug Administration (USFDA), NTIS Issue Number 201304 2012.
- [124] Sheng-Fowler, L., Lewis, A. M., Jr., Peden, K., *Biologicals* 2009, **37**, 190–195.
- [125] Sheng-Fowler, L., Lewis, A. M., Jr., Peden, K., *Biologicals* 2009, **37**, 259–269.
- [126] Mast, T. C., Kierstead, L., Gupta, S. B., Nikas, A. A., Kallas, E. G., Novitsky, V., Mbewe, B., Pitisuttithum, P., Schechter, M., Vardas, E., Wolfe, N. D., Aste-Amezaga, M., Casimiro, D. R., Coplan, P., Straus, W. L., Shiver, J. W., *Vaccine* 2010, **28**, 950–957.
- [127] Zhang, S., Huang, W., Zhou, X., Zhao, Q., Wang, Q., Jia, B., *J. Med Virol.* 2013, **85**, 1077–1084.
- [128] Condezo, G. N., Marabini, R., Ayora, S., Carazo, J. M., Alba, R., Chillón, M., San Martín, C., *J. Virol.* 2015, **89**, 9653–9664.
- [129] Daniell, E., *J. Virol.* 1976, **19**, 685–708.
- [130] Burlingham, B. T., Brown, D. T., Doerfler, W., *Virology* 1974, **60**, 419–430.
- [131] Yang, X., Agarwala, S., Ravindran, S., Vellekamp, G., *J. Pharm. Sci.* 2008, **97**, 746–763.
- [132] Berkowitz, S. A., Philo, J. S., *Anal. Biochem.* 2007, **362**, 16–37.
- [133] St George, J. A., *Gene Ther.* 2003, **10**, 1135–1141.
- [134] Maizel, J. V., White, D. O., Scharff, M. D., *Virology* 1968, **36**, 115–125.
- [135] Sweeney, J. A., Hennessey, J. P., Jr., *Virology* 2002, **295**, 284–288.
- [136] Echavarría, M., Forman, M., van Tol, M. J., Vossen, J. M., Charache, P., Kroes, A. C., *Lancet* 2001, **358**, 384–385.
- [137] Heim, A., Ebnet, C., Harste, G., Pring-Akerblom, P., *J. Med Virol.* 2003, **70**, 228–239.
- [138] Lankester, A. C., van Tol, M. J., Claas, E. C., Vossen, J. M., Kroes, A. C., *Clin. Infect. Dis.* 2002, **34**, 864–867.
- [139] Ma, L., Bluysen, H. A. R., De Raeymaeker, M., Lauryssens, V., van der Beek, N., Pavliska, H., van Zonneveld, A.-J., Tomme, P., van Es, H. H. G., *J. Virol. Methods* 2001, **93**, 181–188.
- [140] Bettonville, V., Nicol, J. T. J., Furst, T., Thelen, N., Piel, G., Thiry, M., Fillet, M., Jacobs, N., Servais, A.-C., *Talanta* 2017, **175**, 325–330.
- [141] Bettonville, V., Nicol, J. T. J., Thelen, N., Thiry, M., Fillet, M., Jacobs, N., Servais, A.-C., *Electrophoresis* 2016, **37**, 579–586.
- [142] Römer, J., Montealegre, C., Schlecht, J., Kiessig, S., Moritz, B., Neusüß, C., *Anal. Bioanal. Chem.* 2019, **411**, 7197–7206.
- [143] Sánchez-Hernández, L., Montealegre, C., Kiessig, S., Moritz, B., Neusüß, C., *Electrophoresis* 2017, **38**, 1044–1052.
- [144] Römer, J., Kiessig, S., Moritz, B., Neusüß, C., *Electrophoresis* 2021, **42**, 374–380.
- [145] Römer, J., Stolz, A., Kiessig, S., Moritz, B., Neusüß, C., *J. Pharm. Biomed. Anal.* 2021, **201**, 114089.
- [146] Dai, J., Lamp, J., Xia, Q., *Anal. Chem.* 2018, **90**, 2246–2254.
- [147] Mack, S., Arnold, D., Bogdan, G., Bousse, L., Danan, L., Dolnik, V., Ducusin, M., Gwerder, E., Herring, C., Jensen, M., Ji, J., Lacy, S., Richter, C., Walton, I., Gentalen, E., *Electrophoresis* 2019, **40**, 3084–3091.
- [148] Kiesel, I., Paulus, M., Nase, J., Tiemeyer, S., Sternemann, C., Rüster, K., Wirkert, F. J., Mende, K., Büning, T., Tolan, M., *Langmuir* 2014, **30**, 2077–2083.
- [149] Lucy, C. A., MacDonald, A. M., Gulcevc, M. D., *J. Chromatogr. A* 2008, **1184**, 81–105.
- [150] Verzola, B., Gelfi, C., Righetti, P. G., *J. Chromatogr. A* 2000, **868**, 85–99.
- [151] American Type Culture Collection (ATTC), *Human adenovirus 5 VR-1516: product sheet*, ID: VR-1516, ATTC, Manassas, VA 2021.